# SPECTROSCOPIC INVESTIGATIONS OF INTRAMOLECULAR RELAXATIONS IN ORGANIC COMPLEX MOLECULES

B. S. NEPORENT
*The State Optical Institute, 199164 Leningrad, USSR*

## ABSTRACT

Some experimental results referring to vibrational and electronic (vibronic) relaxations in organic complex molecules are considered on the basis of simple models. The fundamental role of normal vibrational interactions is shown in the formation of mixed vibrational and vibronic molecular states, determining the dynamics of the absorbed light energy transformations. A convenient classification of the vibrational and vibronic states of molecules is suggested, based only on intramolecular interactions. Some examples of quantitative analyses of absorption and fluorescence spectra relationships are given for rather complicated cases.

In the last few years interest has been aroused in the investigations of energy transformations following light absorption or emission in organic complex molecules. The number of original new experimental studies is increasing and a theory of electronic relaxations in polyatomic molecules is rapidly being prepared. Theoretical results considered in many reviews[1,2] have usually been illustrated by experimental data on polyatomic molecules of medium complexity.

The purpose of this paper is to discuss some typical experimental results related to the processes in complex polyatomic molecules possessing continuous vibronic spectra. The theories based on the initial Born–Oppenheimer states are not always appropriate for describing such systems. We shall introduce a simple model as a basis of our consideration. However, this model permits one to follow the main features of the processes and sometimes to obtain quantitative characteristics of the phenomena.

**1.** Pure vibrational and electronic molecular states of the Born–Oppenheimer scheme exist only in the narrow region near the bottom of deep, isolated potential pits. These states interact and become mixed together when receding from the bottom.

In diatomic and the simplest polyatomic molecules such interactions result in level displacement and variations of transition probabilities. Among these are, for instance, the occasional Fermi resonance[3] (i.e. interaction of vibrational states) and the occasional predissociation after Ittman[4] (i.e. interaction of electronic states in the region of the potential curve crossing

and 'repelling' of the mixed state curves) (cf. *Figure 2* below). The discrete structure of the vibronic and vibrational spectra of the simple molecules under consideration is conserved due to the reversibility of radiationless transitions between the mixed states.

In contrast, in polyatomic molecules radiationless transitions become almost irreversible, that is they acquire a relaxation character. As a result, the potential splitting $\Delta V$ is replaced by the uncertainty $\delta V$ in the $V$ values. The $\delta V$ value is determined by the irreversible transition probability $W^{v}$ into other states, which decreases the duration $\Theta$ of the molecular initial state:

$$\delta V = \frac{1}{2\pi} W = \frac{1}{2\pi\Theta}$$

or, in more convenient form: (1)

$$\delta V \text{ cm}^{-1} = 5 \times 10^{-12} W \text{ s}^{-1}$$

The great number of interacting normal vibrations in complex polyatomic molecules causes the irreversibility and the high radiationless transition probability determining the appearance of diffuse and continuous vibronic spectra and governing the intramolecular processes of absorbed radiation energy transformation. We have already mentioned[5] that the main properties of complex molecules depend specifically upon the rate of vibrational energy redistribution between the normal vibrations, a major part of which form a 'thermal bath' or an 'inner solvent'. Using this property the polyatomic molecules were subdivided[5] into simple ones, in which the bath is isolated, and complex ones, in which it is switched on. In other words in simple molecules $W^{v} < \tau^{-1}$ whereas in complex molecules $W^{v} > \tau^{-1}$, where $\tau$ is the duration of the molecular state under consideration. Using the same feature Fischer and Schlag[6] subdivided the states of polyatomic molecules into communicating and non-communicating ones.

(In further discussion we shall employ the early results[5], some of our later works[7], and also some recent ideas[8-12].)

The above consideration may be illustrated by two simple schemes. There is nothing better now than a geometrical representation of the processes taking place. It is of great importance though to conceive distinctly the limitation of these schemes.

**2.** The vibrational terms of a hypothetical triatomic molecule with $\nu_1$, $\nu_2$ and $\nu_3$ modes are shown in *Figure 1* on the left. The diagram depicts a real structure of vibrational levels excluding a few of their displacements caused by Fermi resonances.

In polyatomic organic molecules the interaction of the three vibrations with many other vibrations results in relaxation level broadening $\delta\nu$, which is customarily assumed to increase with vibrational energy store $Q$. As a consequence, the high levels are overlapped and form an inhomogeneously broadened vibrational state zone. The Fermi resonances fail to be occasional and cover the levels. Strong interactions of normal vibrations make it impossible to separate any one individual state in such a zone.

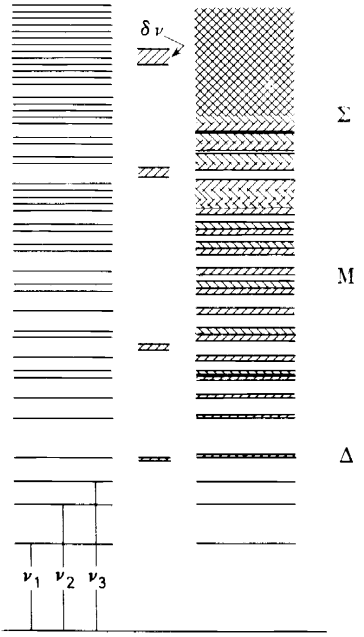


*Figure 1.* The scheme of vibrational levels of triatomic (on the left) and polyatomic (on the right) molecules for three normal vibrations $\nu_1$, $\nu_2$, $\nu_3$. The relaxational broadening $\delta\nu$ is shown in the centre

The width of a latent structure element in this zone is determined by the probability $W^v$ for relaxation[13];

$$W^v = \frac{2\pi}{\hbar}\bar{v}^2\sigma \tag{2}$$

where $\bar{v}$ is the average energy of interactions between the pairs of the initial states, $\sigma = (\mathrm{d}\nu)^{-1}$ is the density of states, and $\mathrm{d}\nu$ is the distance between the neighbour levels. Obviously $\delta\nu = v^2\sigma/\hbar$. Similar expressions are naturally found in all modern theories of electronic relaxations. The principal aim of a theory is the correct selection and calculation of the interaction operator and its matrix element $v$.

In accordance with Ref. 9, we shall call the considered limiting region of the vibrational states, where $\delta\nu \gg \mathrm{d}\nu$, the region of 'mixed vibrations', or the Σ-type region, for brevity. In essence, the assumptions used in the calculation giving equation 2 lose their validity in this region.

The other limiting states of 'independent vibrations' or the Δ-type states are realized in the region of small vibrations[9]. The levels of independent vibrational states are far away from each other. These levels are displaced (to the extent that the radiationless transitions are reversible) and broadened (depending upon the degree of irreversibility of such transitions).

And lastly, the region of intermediate states of the M type is always present.

A convenient criterion for the type of molecular states are the relationships ($2\pi c \approx 2 \times 10^{11}$ cm s$^{-1}$):

$$W^{v}(s^{-1}) \times \sigma(\text{cm}) \ll 2 \times 10^{11} \text{ cm s}^{-1} \text{ state } \Delta$$
$$W^{v}(s^{-1}) \times \sigma(\text{cm}) \approx 2 \times 10^{11} \text{ cm s}^{-1} \text{ state M} \quad (3)$$
$$W^{v}(s^{-1}) \times \sigma(\text{cm}) \gg 2 \times 10^{11} \text{ cm s}^{-1} \text{ state } \Sigma$$

3. The diagram of potential energy surfaces illustrates many molecular features better than the level diagram in *Figure 1*.

In diatomic† molecules the potential-curves' crossing of interacting states (*Figure 2*, the occasional predissociation) gives rise to potential splitting and

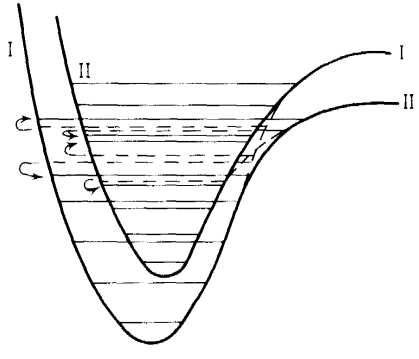


*Figure 2.* Diatomic molecule potential curves: splitting of mixed states and displacement of vibrational levels are shown

level displacement. For polyatomic molecules *Figure 3* shows the projection on planes $V_{I}$, $r_{eI}$ and $V_{II}$, $r_{eII}$ of a pair crossing each other's potential energy hypersurfaces $V_{I}(R_{I})$ and $V_{II}(R_{II})$, belonging to states I and II, the molecule characterizing strong coupling of $v_e$ vibration with the thermal bath. It will be recalled that in this case the figure plane refers only to the projection of multidimensional movements of the depicted point.

In a consideration of the potential hypersurfaces the fact that the interactions of vibrational states in a molecule are due to non-ideal elasticity of some natural coordinates (bond lengths and angles between the bonds) and, therefore, of some normal nuclear coordinates $r_j$ should be taken into account. This results in deviations from the parabolic form of the potentials $V_j$ for corresponding normal vibrations $v_j$. As a consequence, the normal coordinates $r_j$ become non-orthogonal and the vibrations $v_j$ become an-

† The normal molecular coordinates $r_j$ are ascertained from the values of $r_j = 0$ conforming to its equilibrium configuration $R_0 = 0$. A set of the $r_1 \ldots r_j \ldots r_s$ values forms a momentary molecular configuration $R(r_j)$. Frequencies of normal molecular vibrations are $v_1 \ldots v_j \ldots \ldots v_s$, and quantum numbers of the levels populated are $k_1 \ldots k_j \ldots k_s$. A set of values of $k_j$ gives the vibrational molecular state $K(k_j)$. The total vibrational energy store of a molecule is $Q = \Sigma q_i$. The molecular energy is measured in cm$^{-1}$ and denoted by $v$; $v^{00}$ represents the pure electronic energy. The normal vibration potential is $V_j(r_j)$, and the multidimensional one is $V(R)$. The density of the vibrational states is $\sigma$. The values referring to the excited state are denoted by asterisks ($V^*$, $R^* \ldots$) and those of the Franck–Condon states are primed ($V'$, $R' \ldots$).

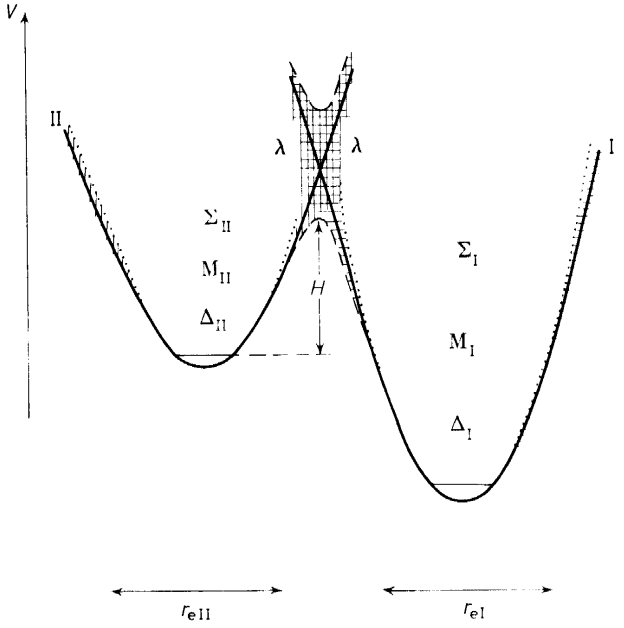


*Figure 3.* Sections through the planes $V_I, r_{eI}$ and $V_{II}, r_{eII}$ of crossing potential energy hypersurfaces of ground partial electronic states I and II

harmonic. This leads to interaction between these vibrations, as a result of which the potential undergoes some splitting and its uncertainty becomes larger, the greater is the number of interacting vibrations. This uncertainty shown in *Figure 3* by the hatched area increases with increasing deviation of the potential hypersurface $V(R)$ (solid curve) from the paraboloid form (broken line).

A geometrical representation of the Σ-type states by means of potential hypersurfaces $V(R)$ can only be maintained if the thickness $\delta V(R)$ of these 'hypersurfaces' is equal to the potential $V$ uncertainty[10, 11]. The uncertainty $\delta V(R)$ exists independently of relaxation processes and moreover it defines their possibility. In geometrical representation the vibrational relaxations are displayed by horizontal displacements of the depicted point inside the hypersurface thickness. Because of a lack of a theory of strong interactions, the thickness $\delta V(R)$ will be treated as a molecular property being subjected to experimental determination, although a precise theory must lead to the potentials $V$ with uncertainty $\delta V$ if it is not self-restricted by assumption of orthogonal normal coordinates and harmonic vibrations.

The width of the levels of the Δ- and *M*-type states is described by the interaction matrix elements $v^{\nu}$ which determine a mean value of $W^{\nu}$ for each $K(k_j)$ vibrational state. The vibronic spectra $\Delta \rightarrow \Delta'$ and $\Delta \rightarrow M'$ are formed as a result of transitions between individual levels (*Figure 4a*). In contrast, the Σ-type regions which cannot be subdivided into separate vibrational states should be described by a set of instantaneous states (configurations),

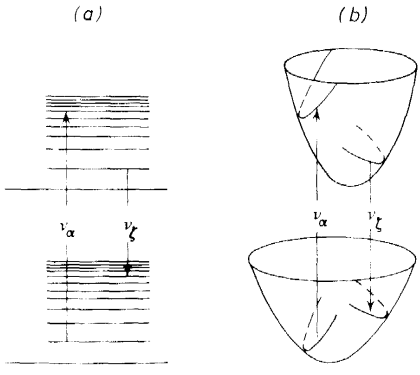


*Figure 4.* The scheme of optical transitions, (*a*) $\Delta \rightarrow \Delta'$ and (*b*) $\Delta \rightarrow \Sigma'$

$R$ being in line with their $\delta\nu(R)$ values. The vibronic spectra $\Delta \rightarrow \Sigma'$ are formed as a sum of transitions from various instantaneous configurations $R$ of the Δ- or M-type initial states into corresponding Franck–Condon ones, $R'$ of the Σ-type states (*Figure 4b*). Here a set of $\delta V(R')$ values for the combination of all optical transitions with the frequency $\nu$ into different instantaneous configurations of the Σ′-type states defines the shape and width of the element of latent vibrational structure of continuous broad bands in configurational vibronic spectra (for more detail see Ref. 10). Such a picture, now universally accepted for complex molecules, was first suggested for diatomic molecules by Vinans and Stueckelberg[14], who used the form $\psi(r) = \delta(r)$ for the wave function of a non-stationary Franck–Condon state in an elementary transition point. Naturally, the authors[14] were unable to introduce an uncertainty $\delta V$ of the potential.

**4.** It is important to emphasize here that the regions of the Δ, M and Σ states on the potential hypersurfaces are not separated by horizontal planes with $V = \text{const}$. The border values depend sufficiently on the instantaneous molecular configuration $R$, and the regions Δ, M and Σ can be peculiarly interlaced. In fact, at a given value of the potential energy $V$, rather small uncertainties $\delta V$ are achieved in the regions of $R$ which correspond to the almost equilibrium energy distribution between all normal vibrations ($r_1 \neq 0, \ldots r_j \neq 0 \ldots r_s \neq 0$). On the other hand, $\delta V$ is fairly high at non-equilibrium configurations ($r_i \neq 0$, $r_{l \neq i} = 0$) but these relationships depend essentially upon the properties of individual vibrations.

Thus, high-frequency stretching vibrations $\nu_l$, often comprising long progressions in discrete and diffuse vibronic spectra and causing the general shape of continuous configurational vibronic spectra, usually exhibit small anharmonicity. Their potentials $V_l$ only slightly deviate from the parabolic one and the values of $W^\nu$ and $\delta V$ in hypersurface cross-sections along $r_l$ are relatively small and increase slowly with increasing $V_l(r_l)$.

Another group comprises the low-frequency bending vibrations $\nu_m$ which are distinguished by large anharmonicity, increasing rapidly with an increase in $V_m(r_m)$ and hence by high activity in the sense of intramolecular interactions,

and consequently by high values of $W^v$ and $\delta V$. These vibrations easily form, at comparatively small values of $V_m$, the subsystems of the $\Sigma$ type with other low-frequency vibrations $v_p$, $v_q$, $v_e$.

It should be noted that Terenin[15] has already considered the bending vibrations to be important stimulators for intramolecular interactions and for molecular level diffusion.

The bending vibrations $v_p$ (they were denoted $v_g$ in Ref. 9) must be mentioned here. These disturb the molecular coplanarity and consequently the $\pi$-electron shell and electronic state, and hence they are parametrically connected with the other vibrations including $v_l$ which do not come into direct anharmonic interaction. Provided that the $v_p$ vibrations take part in the $\Sigma$-type system formed with the other low-frequency modes, they are responsible for the parametric vibronic relaxations including the major part of the molecular vibrations[9].

Among another specific group of vibrations of considerable importance are the bending vibrations $v_e$ associated with normal coordinates $r_e$, and connected with radiationless transitions between the partial electronic states. It is such a coordinate $r_e$ that is used in *Figure 3*. For this reason, as well as the $\Delta$, M and $\Sigma$ zones, the $\lambda$-type region, or transition region of mixed vibronic states which refer to both interacting electronic states (I or II), is shown in *Figure 3*. The vibronic (electronic) relaxations taking place in this region will be discussed below. Note here only that with increasing $V_e(r_e)$ and approaching the transition region $\lambda$, the potential $V$ deviations from parabolic form, as well as the probabilities $W^v$ for vibrational relaxations, increase sharply. This provides the relaxation nature of a radiationless electronic transition I $\leftrightsquigarrow$ II or II $\leftrightsquigarrow$ I, if the density of states is sufficient.

**5.** Consider the experimental spectroscopic evidence associated with vibrational relaxations. These studies follow a general pattern: at first, a molecule undergoes an optical action (absorption or radiation of light), then for a sufficiently short time, $\theta^v = (W^v)^{-1}$, the changes in its vibrational state are either directly observed spectroscopically, or this state is artificially disturbed (molecular collisions, competitive electronic relaxations, repeated radiation effects) and the final results spectroscopically observed.

The probabilities for slow vibrational relaxations in simplest polyatomic organic molecules can be evaluated from the results of resonance fluorescence studies of free gaseous molecules, performed firstly by Kistiakowski and Nelles[16] in benzene, by Pringsheim[17] in anthracene and by Vartanyan[18] in aniline. In recent years, resonance fluorescence has been obtained in many investigations involving the excitation of molecules to some different vibronic levels (Parmenter and Shuyler[19]; Selinger and Were[20]; Spears and Rice[21] in benzene; Quack and Stockburger[22] in aniline; Schlag, Schneider and Chandler[23] by $\tau$ measurements in naphthalene; and Mirumyantz, Vandyukov and Demchuk[24] in anthracene).

The existence of resonance fluorescence indicates that the molecules under discussion are simple ones, namely $W^{v*} < \tau^{-1}$ or $W^{v*} < A + W^{e*}$, where $A$ is the emission probability and $W^{e*}$ is the probability for radiationless electronic transition from the considered state. Using the determined values of $\tau$[21, 23, 25], the probabilities $W^{v*}$ can be calculated as $\approx 10^7\ s^{-1}$ for benzene, $\approx 10^8\ s^{-1}$ for aniline and $\approx 10^4\ s^{-1}$ for naphthalene on excitation in the region

of the first absorption bands. According to Klochkov[26], the resonance fluorescence in anthracene occurs from a special electronic state.

In a consideration of the anti-Stokes band intensities in discharge radiation in diluted vapours of some compounds, Stockburger[27] has recently estimated the ratio of $W^{v*}:A$ for relaxations in the excited molecule from the first vibrational state $k_l = 1$ to the zeroth one. From his estimates it follows that for benzene ($\nu_l = 923\,\mathrm{cm}^{-1}$) $W^{v*} \approx 0.5\,A \approx 10^6\,\mathrm{s}^{-1}$, for toluene ($\nu_l = 936\,\mathrm{cm}^{-1}$) $W^{v*} \approx 5A \approx 3 \times 10^7\,\mathrm{s}^{-1}$ and for naphthalene ($\nu_l = 1435\,\mathrm{cm}^{-1}$) $W^{v*} \approx 20A \approx 10^8\,\mathrm{s}^{-1}$, using the literature values of $A$[18, 28, 29].

The increase in $W^{v*}$ and step-by-step formation of continuous spectra associated with transition into $\Sigma^{*1}$-type states are illustrated by the results[5] of fluorescence studies on β-naphthylamine diluted vapour (*Figure 5*). A change over from excitation by the mercury lines I–III (*Figure 5a*) in the region of diffuse absorption bands ($Q^* = 0$–$3000\,\mathrm{cm}^{-1}$) to excitation by the

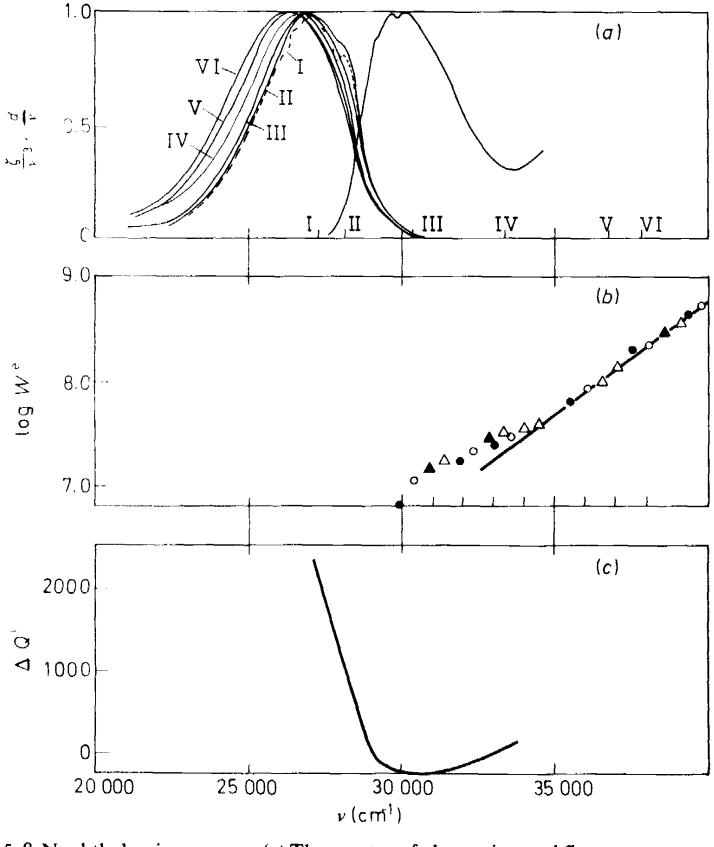


*Figure 5.* β-Naphthylamine vapour: (*a*) The spectra of absorption and fluorescence on excitation by different mercury lines (I–VI); (*b*) The intersystem crossing probability $W_t^{s*}$ as a function of the excitation frequency $\nu_a$ at four temperatures $T$ from 403 K to 466 K[5]; (*c*) The selective energy $\Delta Q^{v*}$ spectrum[49]

IV–VI lines in the region of continuous absorption ($Q^* = 5000$–$10000\ cm^{-1}$) is accompanied by the disappearance of diffuse vibrational structure in the continuous fluorescence spectrum (*Figure 5a*). As $Q^*$ increases, the probability $W^{e*}$ for radiationless transitions, calculated by the measured lifetimes $\eta_\zeta(\nu_\alpha)$ and the fluorescence yield $\tau(\nu_\alpha)$, also exponentially increases (*Figure 5b*). Moreover, an increase of vapour temperature $T$ in the region of small $Q^*$ causes a greater increase in $W^{e*}$ than a relative increase in the frequency $\nu_\alpha$ of the exciting light. In the region of high $Q^*$ the optical ($\nu_\alpha$) and thermal ($T$) ways of increasing $W^{e*}$ are equivalent. Non-equivalency ($\nu_\alpha$, $T$) indicates an incomplete approach of vibrational equilibrium at small values of $Q^*$†. These conclusions are confirmed by independent investigations[33] of the energy transfer in the regions of small and high $Q^*$.

The equivalency ($\nu_\alpha$, $T$) indicates the validity of the condition $\Theta_L^{v*} < \tau$, where $\Theta_L^{v*} = \Theta_1^{v*} + \ldots + \Theta_i^{v*}$ is the characteristic time of the relaxation chain which brings the molecule from the Franck–Condon state to one of vibrational equilibrium. The latter is, in its turn, an initial state for the slower electronic relaxation. In the region of $Q^* = 0$–$3000\ cm^{-1}$ where equivalency ($\nu_\alpha$, $T$) fails to be revealed, apparently $\Theta_L^{v*} \approx \tau \approx 10^8\ s^5$ or $W_1^{v*} \approx W_i^{v*} \approx 10^8\ s^{-1}$. In the region of equivalency ($\nu_\alpha$, $T$), that is at $Q^* = 3000$–$10000\ cm^{-1}$, $\tau \approx 10^{-9}$ s and $\Theta_L^{v*} \approx 10^{-9}$–$10^{-10}$ s. In the region of high vibrational states $\Theta_1^v \ll \Theta_L^{v\,10}$, and therefore one can consider that $W_1^{v*} \approx 10^{10}$–$10^{11}\ s^{-1}$. The values of the vibrational state density $\sigma^*$ for β-naphthylamine may be evaluated as $\sigma^* \approx 10^3\ cm^{-1}$ at $Q^* \approx 3000\ cm^{-1}$ and $\sigma^* \approx 10^7\ cm^{-1}$ at $Q^* \approx 10000\ cm^{-1}$ (by analogy with the data for naphthalene and in accordance with the data[30] for β-naphthylamine). On the basis of equation 3 it follows that the lowest levels ($W^{v*} \times \sigma^* \approx 10^{11} \approx 2\pi c$) belong to M′ states whereas the higher ones ($W^{v*} \times \sigma^* \approx 10^{14}$–$10^{18} \gg 2\pi c$) belong to Σ′ states.

**6.** The faster vibrational relaxations in more complicated molecules have been studied by the method of stimulated emission. Topp, Rentzepis and Jones[34] using a combination of a Kerr cell and an echelon studied, with a resolution of some picoseconds, the development of stimulated emission spectra emitted by the travelling wave in Rhodamine 6G solutions excited by ruby laser second harmonic picosecond pulses. They found (in addition to other results) the 'usual' stimulated emission of Rhodamine 6G similar to that observed under softer conditions of excitation, i.e. appearing from the almost thermalized state, and is developed in $6$–$15 \times 10^{-12}$ s after the excitation.

The kinetics of gain rise in dye solutions pumped by picosecond pulses was measured by Ricard, Lowdermilk and Ducuing[35] by means of a probe pulse passed through the variable delay line. The results of the measurements[35] are relevant to the characteristic time of maximal gain approach or, in other words, to the duration of the relaxation chain bringing the molecule to vibrational equilibrium, being equal to $\Theta_L^{v*} = 8 \times 10^{-12}$ s for Rhodamine

† Using up-to-date procedures, Schlag and Weyssenhoff[30] have recently repeated the earlier[5] measurements of τ. They obtained almost the same results and discussed the applications of some theories of electronic relaxations to these data. Arrhenius formula treatment of the data[5] has been previously conducted by Boudart and Dubois[31], and by Stevens[32], who was compelled to ascribe different values of the molar specific heat of β-naphthylamine to the regions of small and large $Q^*$ values, confirming the incomplete approach of vibrational equilibrium at small $Q^*$.

6G solution in ethanol. The value of $\Theta_L^{\nu*} = 2 \times 10^{-12}$ s has been obtained for Rhodamine B at several frequencies of the probe pulse. On the basis of these data one can evaluate the probability of the first step of the thermalizing relaxation chain in a Rhodamine 6G molecule as $W_1^{\nu*} \approx 10^{12}$–$10^{13}$ s$^{-1}$, and the probability of the last step, which is close to equilibrium distribution, as $W_i^{\nu*} \approx 10^{11}$–$10^{12}$ s$^{-1}$.

A suggestion that the considered relaxations are of an intramolecular nature was obtained in the works of Shilov, Lukomsky and the author[36–38] on the shifts of stimulated emission spectra of dye solutions during the nanosecond pumping monopulses. The phenomenon had been discovered by Bass and Steinfeld[39] and Gibbs and Kellock[40], who ascribed it to relaxation delays in the release of the Franck–Condon levels of the ground state, which populated rapidly in the course of stimulated emission. This spectra shift failed to appear[36–38] in molecules with homogeneously broadened relaxational vibronic spectra (e.g. 3,6-tetramethyldiaminophthalimide, *Figure 6*) and in chlorine–aluminium phthalocyanine which behaves similarly to vanadium phthalocyanine in experiments[41] on photobleaching and exhibits

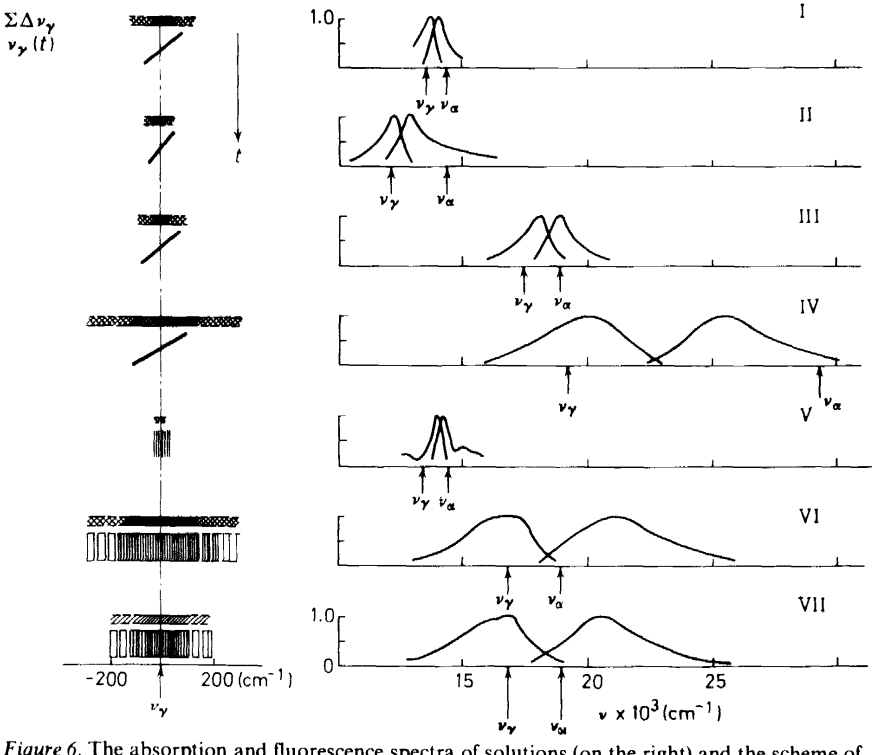


*Figure 6.* The absorption and fluorescence spectra of solutions (on the right) and the scheme of their stimulated emission spectra shift during the pumping by a laser monopulse (on the left). Shown for each substance are, the summary stimulated emission spectrum (at the top), and its development in time (at the bottom). I, cryptocyanine; II, 3,3-diethylcarbocyanine iodide; III, Rhodamine 6G; IV, 3-amino-*N*-methylphthalimide; V, phthalocyanine–ClAl; VI, 3,6-tetramethyldiamino-*N*-phthalimide; VII, 3-dimethylamino-6-methylamino-*N*-methylphthalimide

homogeneously broadened diffuse levels with a width $\delta\nu \approx 500\,\mathrm{cm}^{-1}$. In the case of inhomogeneously broadened configurational spectra (e.g. 3-amino-*N*-methyl-phthalimide, Rhodamine 6G, etc., *Figure 6*) the shift is observed, with the instantaneous position of stimulated emission spectrum maxima following the pumping intensity. A comparison of the spectral shift kinetics for Rhodamine 6G on pumping by a 20–50 ns monopulse and a picosecond pulse train showed the triplet–triplet absorption to be insufficient for this substance. These facts suggest the relaxational character of the phenomenon. The existence of spectral shifts of Rhodamine 6G in fluid (ethanol) and viscous (glycerin) solvents at $T = 160$–$420\,\mathrm{K}$ (including solid ethanol) showed the intramolecular nature of the phenomenon and the minor importance of intermolecular relaxation. The duration of the relaxation processes responsible for the spectral shifts was estimated[36, 38] as $\Theta_L^{\nu} \approx 10^{11}$–$10^{12}\,\mathrm{s}^{-1}$.

The probabilities $W^{\nu}$ for vibrational relaxations may also be calculated from the results of investigations on photobleaching in a narrow absorption spectral region near the powerful irradiation frequency ('hole burning'); this has been noticed and studied by Spaeth and Sooy[41], and Giuliano and Hess[42]. According to the data of these papers, the 'hole' width $\delta\nu$ for cryptocyanine solutions in methanol upon sufficient powerful radiation is within the limits $1 < \delta\nu < 60\,\mathrm{cm}^{-1}$, which is adequate to the values of $W^{\nu *} + W^{\nu} \approx 10^{11}$–$10^{13}\,\mathrm{s}^{-1}$. It is necessary to note, however, that the investigations of Razumova *et al.*[43] failed to provide support for the hole-burning effect. Photobleaching spectra evidently need to be further investigated and analysed.

7. Turning to the formation of diffuse and continuous vibronic spectra of an isolated polyatomic molecule, consideration should be first of all given to band broadening by overlapping lines of rotational structure of individual vibronic transitions. A case of a relatively broad band is shown in *Figure 7* for the transition $\nu^{00}$ in an aniline molecule according to Christoffersen, Hollas and Kirby[44]. It is obvious that for diffuse structure formation the band peculiarities having a width of 0.5–5 $\mathrm{cm}^{-1}$ must be smoothed away. As stated above, values of vibrational relaxation probabilities of $W^{\nu} \approx 10^{12}$–$10^{13}\,\mathrm{s}^{-1}$ ($\delta\nu \approx 5$–$50\,\mathrm{cm}^{-1}$), quite sufficient for diffuse band formation, can be obtained. However, as well as the mechanism of relaxation broadening[9,33,45],

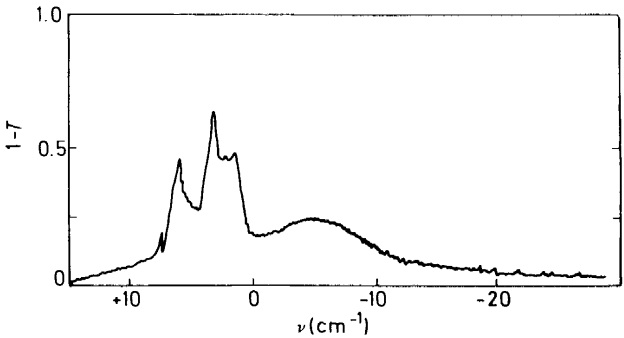


*Figure 7.* The rotational contour of the aniline vibronic spectrum band $\nu^{00}$ according to Ref. 44

another mechanism of sequence congestion suggested by Byrne and Ross[46] is possible. The diffuse maxima in a vibronic spectrum are due to overlapping of the members of sequences formed by non-active $v_q$ vibrations[46] (scheme at the bottom of *Figure 8a*). The overlapping ensures that the distance

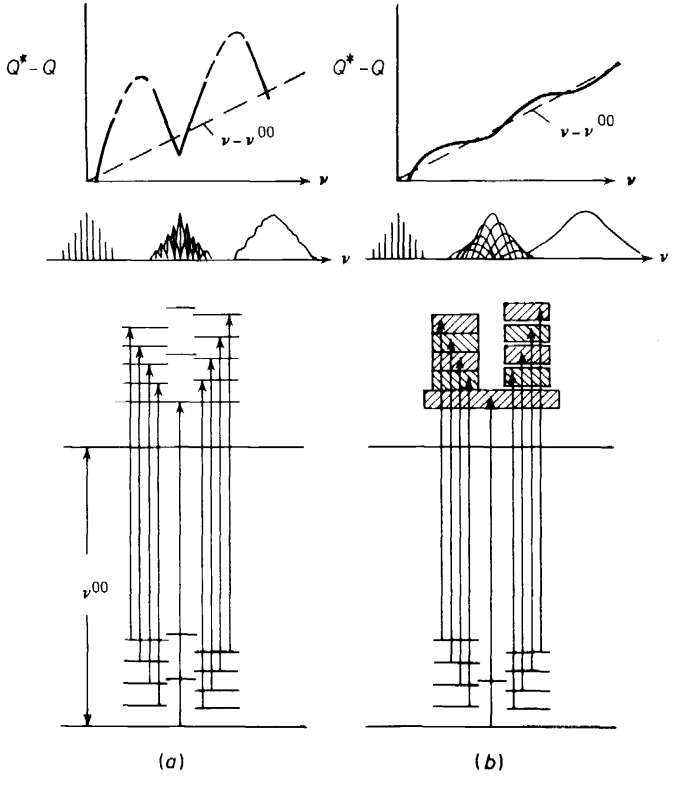


*Figure 8.* (*a*) The scheme of diffuse bands formation due to sequence congestion[46]. At the bottom — the scheme of transitions; in the middle (from left to right) — the scheme of diffuse band formation as a result of rotational structure overlapping; at the top — the dependence of the excited state vibrational energy $Q^*$ on the absorpting quantum frequency $\nu_a$.
(*b*) Simultaneous action of sequence congestions and moderate relaxational broadening

between members of the sequence, determined by the difference in the $v_q$ values in combining electronic states, is small compared to the peculiarities of their envelope rotational structure. The existence of several sequences facilitates the overlapping. The diffuse spectral maximum formation is shown in the middle part of *Figure 8a*.

It should be emphasized that in the case of sequence congestion the vibrational energy $Q^*$ of an excited molecule undergoes pronounced periodical changes, with the exciting light frequency $\nu_a$ varying gradually. In this case the minimal values of $Q^*$ correspond to maxima in the diffuse band of sequence congestion (top of *Figure 8a*). Similar correlations naturally take place also for radiationless transitions, which depend on the $Q^*$ values.

In practice, the vibronic spectra with diffuse maxima can be realized under the joint action of relaxation broadening[9, 33, 45] and sequence congestion[46]. Such a system is illustrated in *Figure 8b*. Members of the sequence are broadened and considerably overlapped. The diffuse maxima are broadened as well, and the periodical variations in $Q^*$ along the spectrum are smoothed over as a result of the members overlapping and of the growth in the probability $W^v$. As the relaxation broadening $\delta\nu$ increases due to strengthening of the vibration interactions, the diffuse maxima also broaden and overlap, and the periodical variations in $Q^*(\nu_\alpha)$ disappear. Further increasing of $\delta\nu$ causes the broad diffuse spectra $\Delta \rightarrow M'$ to change into continuous ones $\Delta \rightarrow \Sigma'$, which have a different mechanism of formation (*Figure 4b*).

It is the character of the function $Q^*(\nu_\alpha)$ that is the criterion for the mechanism of formation of diffuse vibronic spectra. The sequence congestion mechanism is connected with the periodic function $Q^*(\nu_\alpha)$, but the relaxation one is connected with smoothed dependence $Q^*(\nu_\alpha)$. Some years ago Borisevich and Tolkachev[47, 48] introduced a concept of 'selective energy' $\Delta Q^v$ (our designation) estimating it as:

$$\Delta Q^v = \bar{Q}^* - \bar{Q} - (\nu - \nu^{00}) = \frac{d}{d[(T)^{-1}]} \ln I_\nu(T) \qquad (4)$$

and suggested a method for its experimental determination from the temperature dependence of absorption (or fluorescence) spectra. In equation 4, $\bar{Q}^*$, $\bar{Q}$ are the mean values of the vibrational energy of the excited and ground states, and $I_\nu$ is the intensity of the spectrum ($\alpha_\nu$—in absorption, $\zeta_\nu$—in emission). We continue to follow designations given in a series of papers[8–12].

*Figure 9* illustrates the spectra of selective energy of excitation $\Delta Q^{v*}$ for

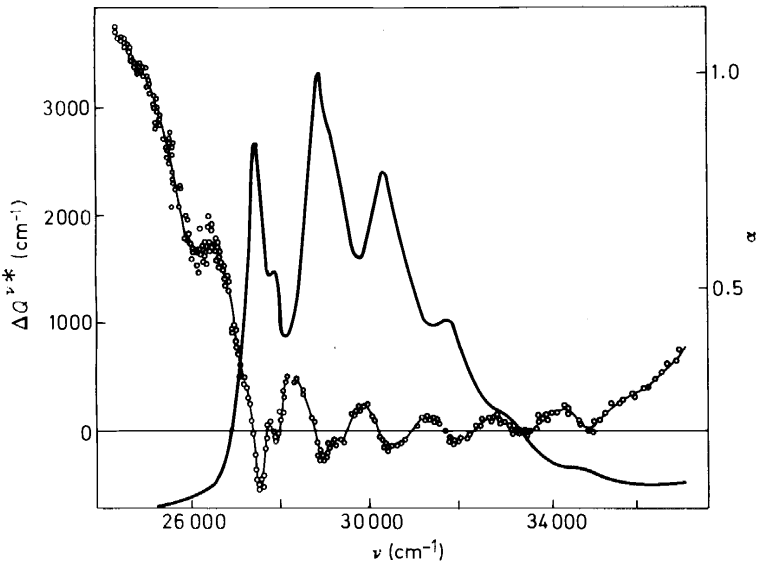


*Figure 9.* The spectra of absorption α and of selective energy of excitation $\Delta Q^{v*}$ for anthracene vapours[49]

anthracene vapours obtained from the temperature dependence of absorption[49]. The structure of the $\Delta Q^{v*}$ spectrum reproduces the details of the $\alpha_v$ spectrum and, according to the above considerations, the diffuse band maxima $\alpha_v$ are in line with the minima $\Delta Q^{v*}$. It is obvious that the diffuse maxima in the anthracene vapour spectrum are formed mainly as a result of sequence congestion.

The results of Weyssenhoff and Krauss[25], who measured the probability $W_t^{e*}$ of intersystem crossing of the excited aniline molecules which is strongly dependent on $\alpha_v$, should be explained in the same way. The spectra of $W_t^{e*}$ shown in *Figure 10* reproduce the absorption spectra $\alpha_v$ structure, with maxima $\alpha_v$ corresponding to minima $W_t^{e*}$.

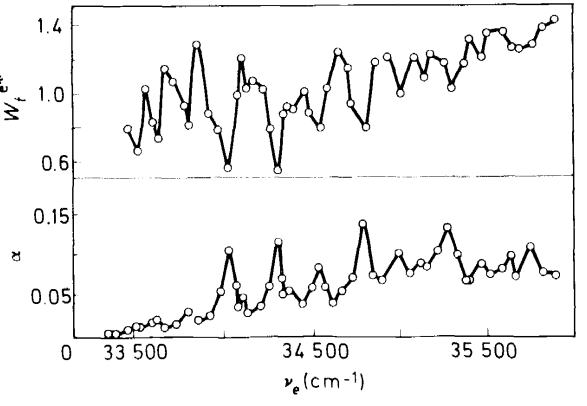


*Figure 10.* The spectra of absorption α and of intersystem crossing probabilities $W_t^{e*}$ in aniline vapour[25]

With β-naphthylamine, which is more complicated than anthracene, the vibrational structure traces in the first absorption band fail to show themselves in the limits of the experimental errors in the spectrum $\Delta Q^{v*}$, which is found to be a smooth curve[47] (*Figure 5c*). In this case the diffuseness of the absorption spectrum seems to be mainly a result of relaxation processes. The authors[46,47] have pointed to the fact that a curve $\Delta Q^{v*}$ rising on the side of low frequencies is determined in all cases by the necessity of an energy-lack compensation in the anti-Stokes region of the absorption spectrum. A slight increase in the values of $\Delta Q^{v*}$ on the side of high frequencies is likely to be caused by the Franck–Condon principle or the second band influence.

**8.** Typical continuous vibronic spectra of polyatomic molecules are given for 3-aminophthalimide and 3,6-tetradimethylaminophthalimide in *Figures 11a* and *12a*[45,50], where the equivalency ($\nu_\alpha$, $T$) in the whole region of the first absorption band was shown by Borisevich and the author. Together with the smooth structureless curves $\Delta Q^{v*}$ (from Ref. 48) in *Figures 11b* and *12b* this indicates that these continuous spectra are formed mainly by relaxation processes. The intramolecular nature of these relaxations has been

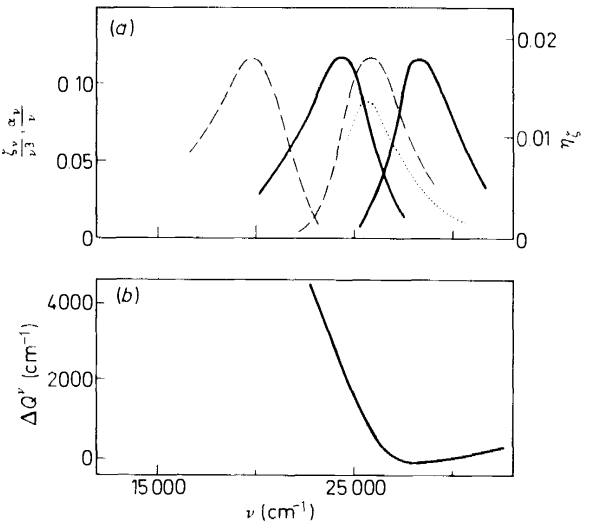


*Figure 11.* 3-Aminophthalimide. (*a*) The absorption and fluorescence spectra of the vapour (— ——) and solution (– – – –), as well as of the fluorescence yield $\eta_\zeta$ of the vapour (·····)[45,50] (*b*) The spectra of selective energy of excitation $\Delta Q^{\nu *}$ of the vapour[48]

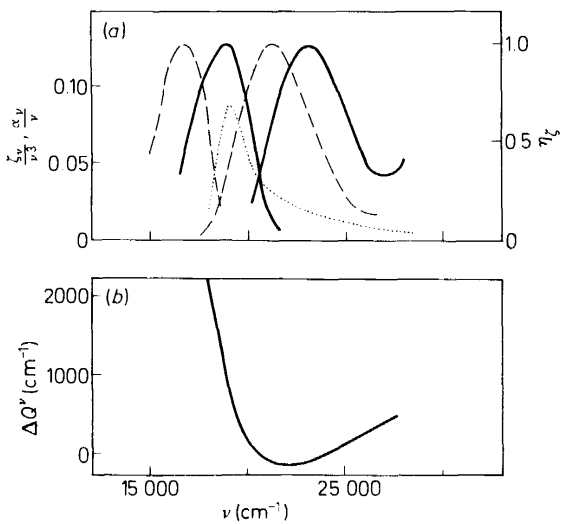


*Figure 12.* 3,6-Tetramethyldiaminophthalimide. (*a*) The absorption and fluorescence spectra of the vapour (— ——) and solution (– – – –), as well as of the fluorescence yield $\eta_\zeta$ of the vapour (·····)[45,50]. (*b*) The spectra of selective energy of excitation $\Delta Q^{\nu *}$ of the vapour[48]

proved[51–53]. The conservation of the continuous character of the absorption ($\alpha_\nu$) and fluorescence ($\zeta_\nu$) spectra was shown for the family of substituted phthalimides in the change from diluted vapour to solution through the critical state. With the considerable change in their position the spectra of 3-aminophthalimide also conserve their width and symmetry ($\Delta\nu_\alpha \approx \Delta\nu_\zeta \approx$ const.) and the spectra of 3,6-tetramethyldiaminophthalimide maintain a peculiar width dependence on their maxima position ($\Delta\nu = C\nu_{max}^2$ for both $\alpha$ and $\zeta$ spectra). On the basis of these relationships, the spectra of 3-aminophthalimide have already been referred to as inhomogeneously broadened configurational ones, and the spectra of 3,6-tetramethyldiaminophthalimide as homogeneously broadened relaxational ones[45, 54] (by the terminology accepted here).

The vibronic interactions resulting in considerable broadening of the 3,6-tetramethyldiaminophthalimide spectra will be discussed in the next section. Here we will direct our attention to the inhomogeneously broadened spectra of 3-aminophthalimide and other similar molecules. In these cases the optical transitions of all frequencies $\nu$, including $\nu \approx \nu^{00}$, obviously lead the molecules into Franck–Condon states of the $\Sigma'$ type. This can only occur if the equilibrium configurations $R_0$ and $R_0^*$ of the molecule in the ground and excited electronic states differ considerably, except for the normal coordinates $r_l$, also in the coordinate $r_m$ (or in $r_p$ or in the group of the $r_m$ and $r_p$ coordinates) of the bending vibrations $\nu_m$ and $\nu_p$, which are distinguished by high anharmonicity even at low $V_m$ and $V_p$ (see Section 4). Such a possibility is realized, for instance, with low rigidity of a conjugated band chain (polyene type) or with active substituent groups (analogous to $NH_2$) injected into rigid aromatic molecules. These or other active groups connected with the $\pi$-electron system cause the substantial difference between $R_0$ and $R_0^*$ (see *Figures 17* and *18*, p. 132) as a consequence of charge-transfer transitions.

The shape of continuous configurational vibronic spectra depends upon the equilibrium configuration difference $R_0^* - R_0$ of the molecule as well as on the shapes of its potential energy hypersurfaces $V(R)$ and $V^*(R)$. The relationships between the absorption and fluorescence spectrum shapes will be considered in Section 14. The importance of the latent vibrational structure investigations in continuous vibronic bands, that is homogeneously broadened elements, which form in the mutual overlapping of such bands, should be emphasized. In terms of relaxational representations, these investigations involve a study of the characteristic times $\Theta^{\nu'}$ of vibrational relaxation in the Franck–Condon states, whereas in terms of potential hypersurfaces they consist of a study of the thicknesses $\delta V_\Sigma = \delta V(R')$, that is the uncertainty of the $V(R')$ values. These studies have been considered above in Sections 5 and 6 for a series of molecules, and some data for 3-aminophthalimide are given there.

In addition, the values of $W_\Sigma^{\nu*}$ can be obtained for a 3-aminophthalimide molecule in a similar way to those of β-naphthylamine since $W_\Sigma^{\nu*} > \tau^{-1}$. Very small values of $\tau$ connected with small values of the fluorescence yield $\eta_\zeta$ could not be measured, and can be determined from $\tau = \tau_\alpha \times \eta_\zeta$ using the values of the intrinsic lifetime $\tau_\alpha = 4 \times 10^{-8}$ s, calculated from the absorption spectra (Strickler and Berg[55]), as well as the reported values of $\eta_\zeta$[50]. At $t = 216°C$ these data lead to $\tau = 6 \times 10^{-10}$ s and $\tau = 4 \times 10^{-11}$ s,

when $\nu_\alpha = 27250\,\text{cm}^{-1}$ and $\nu_\alpha = 31930\,\text{cm}^{-1}$. From this it follows that $10^{11}$–$10^{12} < W_\Sigma^{\nu *} < 10^{12}$–$10^{13}\,\text{s}^{-1}$.

Some information about the inner structure of continuous vibronic bands, especially when they are formed with the participation of non-symmetrical vibrations, might be obtained from the investigations on the polarization of luminescence of relevant compounds. Unfortunately, these investigations are rather complicated by intermolecular relaxation processes which are present in viscous solutions. Marek[56] observed a stepwise decrease in the degree of polarization $P$ along the absorption spectrum of a number of dyes (see, e.g. *Figure 13*) and explained it by the appearance of a vibronic band

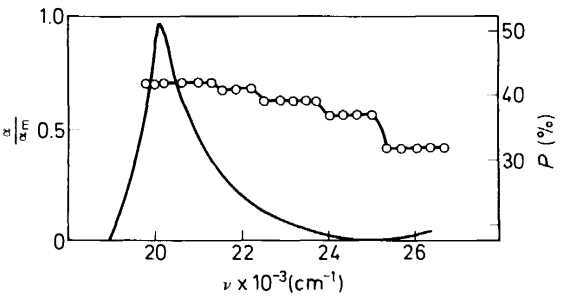


*Figure 13.* Fluorescence polarization spectrum of fluorescein solutions[56]

inner structure. According to the results of Sevchenko, Gurinovich and Sarzhevskii[57], the polarization spectrum of fluorescence of 3,6-tetramethyldiaminophthalimide represents a horizontal line, unlike those of 3-aminophthalimide and other compounds which have the configurational spectra. Irrespective of the discussions of the reasons of the dependence of $P$ on $\nu_\zeta$ this dependence suggests the homogeneous broadening of the 3,6-tetramethyldiaminophthalimide spectra, contrary to the opinion of these authors[57]. In this case the dependence of $P$ on $\nu_\alpha$ is associated with the influence of the near second absorption band.

**9.** To analyse the relaxational spectra let us consider again a cross-section of the potential hypersurfaces of the excited states I* and II* along the coordinates $V_\text{I}^*$, $r_{e\text{I}}^*$ and $V_\text{II}^*$, $r_{e\text{II}}^*$ (with the others $r_{i\neq e}^* = 0$) shown in *Figure 14*. The projections of some relaxational processes and optical transitions are illustrated here as well. The solid arrows of optical transitions denote Franck–Condon states along the coordinate $r_{e\text{I}}^*$, and the dashed ones show the projections of the Franck–Condon instantaneous configurations $R_\text{I}^{*\prime}$ which are out of the schematic plane and are associated with the excitation of vibrations along the other coordinates. (All the relationships under consideration might be completely maintained in the case of the ground states I and II shown in *Figure 3* and in optical transition from higher states). For simplicity, the coordinate $r_{e\text{I}}^*$ is supposed to be associated with the electronic relaxation in the zone of crossing of the hypersurfaces I* and II*

and also, as a result of optical activity of the vibrations $v_e^*$, to determine the shape and character of the configurational vibronic band. Such a case takes place for the pyrazine molecule (see below, next section), though, usually, these coordinates ($r_e$ and $r_l$) are far different.

The vibronic spectrum connected mainly with small vibrations of the coordinate $r_{el}$ in $R_{0l}^* - R_0$ (case *a* in *Figure 14*) is formed in the transitions

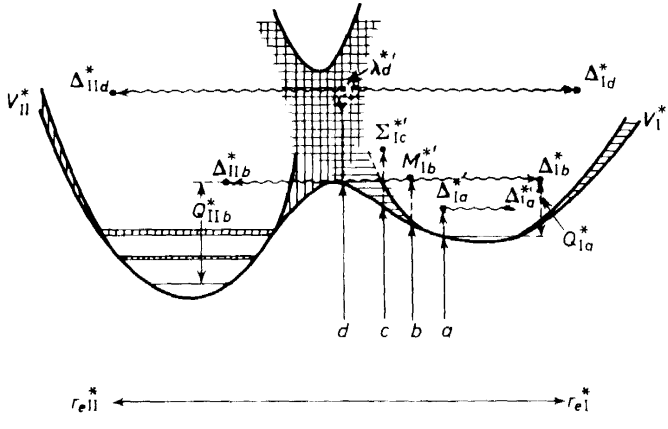


*Figure 14.* Sections along the planes $V_I^*, r_{el}^*$ and $V_{II}^*, r_{eII}^*$ of crossing potential energy hypersurfaces belonging to the excited partial electronic states I* and II*

$\Delta \rightarrow \Delta'$ and is discrete in character. Here $R_0$, $R_{0l}^*$ are the equilibrium configurations of the initial (not shown in *Figure 14*) and final (I*) electronic states. With an increase of the difference $R_{0l}^* - R_0$ (comprising also the changes of the relaxationally active bending coordinates $r_m$), the diffuse and continuous configurational spectra $\Delta \rightarrow M'$ and $\Delta \rightarrow \Sigma'$ are formed (cases *b* and *c* in *Figure 14*). Finally, at large differences in the values of $R_{01}^*$ and $R_0$ along the coordinate $r_e$, now being active in the sense of electronic relaxations (case *d* in *Figure 14*), the optical transitions of the $\Delta \rightarrow \lambda'$ type take the depicted point to the region of mixed vibronic states. Homogeneous broadening in the $\lambda$-type zone can exceed (on strong interaction) the configurational width of the vibronic spectrum which is decreased owing to the small slope of the potential hypersurface conventional boundary (lower curve). In this case the homogeneously broadened vibronic relaxational spectra are formed and these have been detected even by peculiar width correlations[45]. Relatively narrow configurational distribution can appear only at these spectrum sides, just as small relaxational homogeneous broadening can appear at the sides of configurational inhomogeneously broadened continuous vibronic bands. In *Figure 12* (see above) the relaxational vibronic spectra of 3,6-tetramethyldiaminophthalimide are shown with the width $\Delta\nu = 5000\,\text{cm}^{-1}$ corresponding[45] to the electronic relaxation probabilities $W_r^{e*} \approx 10^{15}\,\text{s}^{-1}$. Such high $W^e$ values were also proposed by Hochstrasser and Marzacco[58] to explain the relaxational bandwidths of dimethylpyrazine and diazophenanthrene.

A value of $W^e \approx 10^{15}\,s^{-1}$ should not be thought of as too high, if one considers that the probabilities of intersystem crossing may be as high as $W_t^{e*} \gg A$ or $W_t^{e*} \approx 10^{11}$–$10^{12}\,s^{-1}$ in molecules with high values of phosphorescence yields $\eta_\chi \approx 1$, and that according to Kasha[59] the intersystem limitations which decrease the probability for electronic relaxations may be as small as $10^{-6}$.

The first oddity which classified the relaxational spectra as a separate group[45], was the strange fact that their width could be satisfied for all absorption and fluorescence spectra under all conditions by the above-mentioned relationship: $\Delta\nu = C\nu_{max}^2$ in contrast with the little affected width of inhomogeneously broadened configurational spectra. The relaxational spectra always belong to molecules which are the most complicated of an homological series and, therefore, which possess active and unsymmetrical substituent groups. This is illustrated in *Figure 15*, where the spectra of some

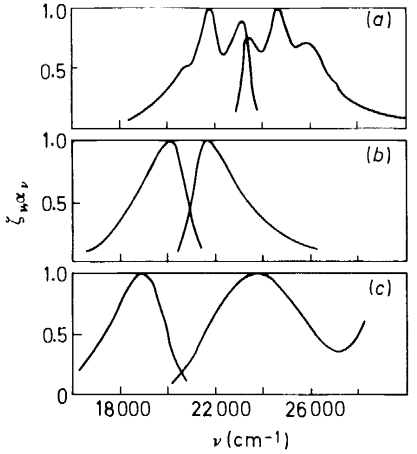


*Figure 15.* The absorption and fluorescence spectra of some aminoacridines in solution[45]: (*a*) 9-aminoacridine; (*b*) 3,6-diaminoacridine; (*c*) 3-aminoacridine

aminoacridines are shown[45]. The last members of this family of compounds exhibit relaxational spectra, as do those of the family of phthalimidies[36] (compare *Figures 11* and *12*), of the triphenylmethane dyes[60,61] and of the rhodamines[62]. The relaxational spectra differ from inhomogeneously broadened configurational ones by a peculiar position of the inversion frequency $\nu_i$ (cf. Section 14 below), by the absence of stimulated emission spectra shifts[36] (see *Figure 6*) and by the characteristic property of the polarization fluorescence spectra, mentioned in Section 8. The features of these spectra have been discussed[7,8,11,54].

**10.** Returning to *Figure 14*, it will be recalled that in the processes of direct and inverse vibronic transitions the initial states of Δ type are formed by relaxational processes from Franck–Condon states of different types. Provided the Franck–Condon state formed in the vibronic optical transitions

is situated below the barrier $H$ (case *a*, state $R^{*\prime}_{Ia} = \Delta^{*\prime}_{Ia}$, *Figure 14*) the thermalizing chain (wavy arrow) comprises only the vibrational relaxations, and the inverse optical transitions occur from the equilibrium configuration $R^{*}_{sI}(Q^{*}_{Ia}) = \Delta^{*}_{Ia}$ lying out of the figure plane, which is in equilibrium in vibrational energy and quasi-stationary with respect to the stationary electronic state II*. When the energies of the Franck–Condon states are above the barrier $H$ (see, e.g., case *b*, *Figure 14*), a competition of relaxational transitions takes place into two vibrational equilibrium states $R^{*}_{sI}(Q^{*}_{Ib})$ and $R^{*}_{sII}(Q^{*}_{IIb})$, belonging to different electronic states I* and II*. The probabilities for each individual vibrational or vibronic relaxation depend in general not only on the vibrational energy $Q^{*}$ store, but also (sometimes to a greater extent) on the instantaneous configurations $R$. Hence, the first rapid chains of vibrational relaxations can give rise to non-equilibrium distribution of molecules between the states $R^{*}_{sIb}$ and $R^{*}_{sIIb}$ (or $\Delta^{*}_{Ib}$ and $\Delta^{*}_{IIb}$). The equilibrium distribution which depends only on the values of $Q^{*}_{Ib}$ and $Q^{*}_{IIb}$ can be set up later on as a result of slower fluctuational vibrational relaxations and vibrational movements, bringing the molecule from the thermalized states $\Delta^{*}_{Ib}$ and $\Delta^{*}_{IIb}$ to the $\Lambda$ region of transition states and of subsequent electronic relaxations. It is clear that such processes are possible if the characteristic time $\Theta^{e*}_{I,II}$ of transitions between the thermalized states $\Delta^{*}_{Ib}$ and $\Delta^{*}_{IIb}$ is considerably smaller than the duration $\tau$ of the states I*–II* which depends on transitions to other excitations, i.e. $\Theta^{e*}_{I,II} \ll \tau$. The probabilities and rates of the relaxational processes under consideration are a subject of the theory of monomolecular reactions, which has to be a part of the theory of polyatomic molecular structure.

As an example, it should be noted here that according to Baba and Hiroaki *et al.*[63], the fluorescence ($S^{**} \rightarrow S_0$) from the second excited level of pyrene, excited by large quanta ($S_0 \rightarrow S^{**}$ and $S_0 \rightarrow S^{****}$) occurs mainly after a rapid ($10^{-12}$ s) transition to high vibrational states of the first excitation S* and a further slower ($10^{-8}$ s) population of the second excitation S**. A rate correlation of the direct and inverse radiationless transitions $S^{*} \leftrightsquigarrow S^{**}$ corresponds approximately to the densities of the states $\sigma^{*}$ and $\sigma^{**}$ at the level of excitation, and the system is thermalized[63]; this is favoured by a small probability of optical transition $S^{*} \rightarrow S_0$.

Contrary to the above case, Galanin and Chizhikova[64, 65], who obtained the fluorescence spectra $S^{**} \rightarrow S_0$ from the second excited level of Rhodamine 6G which had intense vibronic bands, pointed out that the radiationless transition probability $W^{e}_{q}{}^{**} \approx 10^{13}\ s^{-1}$, determined by them from the values of quantum yield ($\eta_{\zeta(II \rightarrow 0)} \approx 10^{-5}$) and intensity of the absorption band ($A_{0-II} \approx 5 \times 10^{7}$), exceeds the vibrational relaxation probability, being for example $W^{v*} \approx 10^{11}$–$10^{12}\ s^{-1}$ for the S* level. These authors[65] mentioned that the non-equilibrium of the initial vibronic level system appears to determine a surplus broadening of the fluorescence band $S^{**} \rightarrow S_0$ compared with the absorption band $S_0 \rightarrow S^{**}$. (However, the possibility that the vibrational relaxation probability $W^{v**}$ in the second excited state may exceed the probability $W^{v*}$ in the first excited state is not excluded.)

**11**. Before considering some electronic relaxation features it should be pointed that the conventional term 'electronic' is not precise enough when used in reference to the complicated process of variations in molecular electronic structure together with variations in nuclear configuration to form

one self-consistent state. As we have repeatedly mentioned, in fact, these relaxations should be termed 'vibronic' relaxations.

These processes occur in the region of crossing of the potential hypersurfaces which forms the $\lambda$-type zone of transition mixed vibronic states (*Figures 3* and *14*) or the 'bottle neck' associating the interacting states. Such a 'neck' can comprise the variations of some normal coordinates. This is suggested in *Figure 16*[66, 67] which represents the variations in the molecular configura-

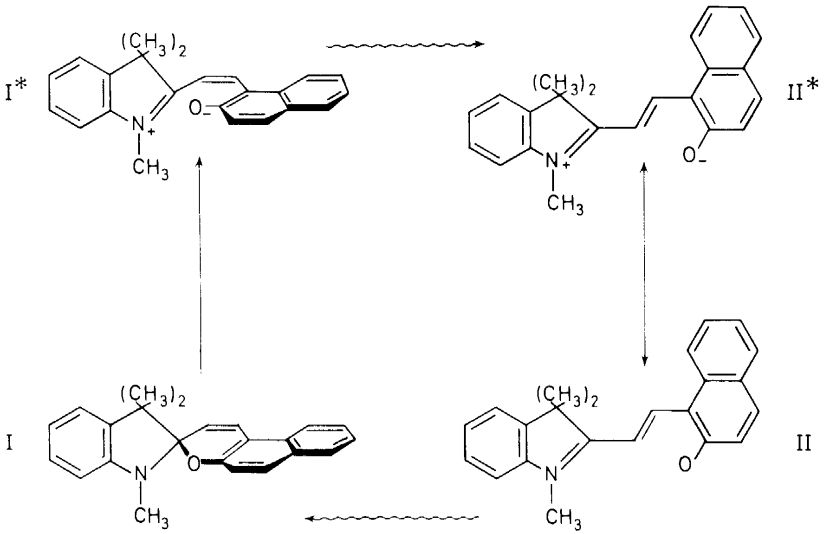


*Figure 16.* Equilibrium configurational changes in electronic rearrangements (wavy arrows) following the electronic transitions (straight arrows) in the spiropyrane molecule[8, 66, 67]

tion of spiropyrane during vibronic relaxations of the electronic rearrangement type[8, 11], following the electronic transitions. Here an electron transfer in an optical transition is followed by changes in the angles and lengths of several bonds. One part of the molecule makes a half-turn and forms (or destroys) the coplanar nuclear configuration. These changes are accompanied by further electronic structure rearrangement and formation of self-consistent stationary states. The scheme of the potential hypersurface cross-sections along one of the normal coordinates, associated with the turning of part of the molecule, is shown in *Figure 17*[8]. Apparently, such systems must be described by the four-level scheme of electronic states; this necessity has been noted[45, 54] and considered in detail[8, 11].

In connection with the four-level scheme it should be especially emphasized that, in spite of the fact that the existence of several partial electronic excited states $S_i^*$ (for instance, $n\pi$ and $\pi\pi$, etc.) is now generally recognized, the admission of the existence of some similar partial ground states $S_{0i}$ meets a psychological barrier, although the necessity for their existence arises from

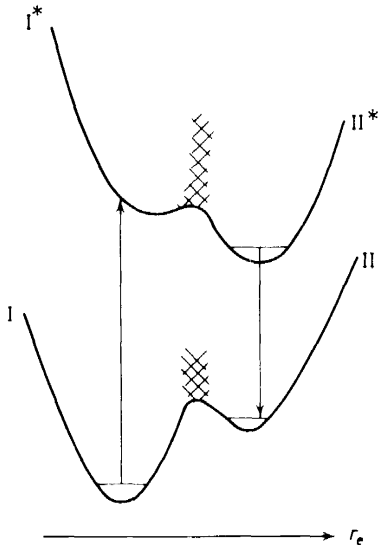


*Figure 17.* Potential hypersurface cross-sections for the transitions in a spiropyrane molecule[8]

many facts and considerations[8,45]. Notice here that provided these states cannot be sometimes considered, in the chemical sense, as real isomers, because of their short lifetime (up to $10^{-12}$–$10^{-15}$ s), they play an important role in spectroscopy.

There are many experimental results which illustrate the peculiar importance of some normal coordinates in the formation of the transition zone as a channel for electronic relaxation. The data of the investigations of Spears and Rice[21] (*Figure 18*) illustrate, for example, an increased influence of the bending out-of-plane vibrations (especially $\nu_{1\sigma} = 243\,\text{cm}^{-1}$ in the

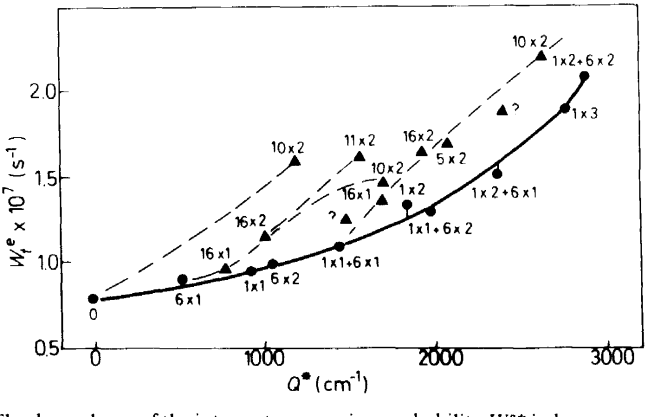


*Figure 18.* The dependence of the intersystem crossing probability $W_i^{e*}$ in benzene vapour on the vibrational energy and on the type of excited vibrations[21] (———, excitation of plane vibrations; – – – –, additional excitation of bending vibrations)

excited state) on the intersystem crossing probability $W_t^{e*}$ in a benzene molecule. The influence of the out-of-plane vibrations of the CHO groups on the interaction of the $n\pi$ and $\pi\pi$ states of aromatic carbonyl compounds was shown by Lim, Li and Li[68] from a dependence of the spectra upon a number of factors. A particular activity of the bending out-of-plane vibrations $\nu = 920\,\mathrm{cm}^{-1}$ of a pyrazine molecule in the mixing of several electronic states should be noted. This was shown by Innes *et al.*[69, 70], Ito and Suzuka *et al.*[71] and Kalantar *et al.*[72] by analysis of the vibronic spectra, by the appearance of this antisymmetrical vibration in the long progression of the fluorescence spectra and by an anomalously rapid increase in intensity of the $920\,\mathrm{cm}^{-1}$ Raman line, with increasing frequency of the excited radiation in the pre-resonance region. Such an anomalous dependence had been predicted in Albrecht's theory[73].

The analysis of similar effects in pre-resonance scattering is very important for molecules having continuous or strongly diffused vibronic spectra. Such investigations enable essential information on vibronic interactions, which is not displayed directly in the vibronic spectra of these molecules, to be obtained.

It has been mentioned above (cf. Section 4) that distortion of the potential hypersurfaces in the regions adjacent to the $\lambda$ zone of their crossing results in a considerable increase in the uncertainty $\delta V(R)$ of the potential $V(R)$. This facilitates the formation of the $\Sigma$-type states, which provide the relaxational nature of the radiationless transitions I $\leftrightsquigarrow$ II (*Figure 14*). The magnitudes of these disturbances, as well as of the uncertainty in the crossing zone (the $\lambda$-type region in *Figure 3*) are determined by the power of the interaction of the electronic states I and II. In simple molecules these interactions may be weakened by the symmetry and multiplicity limitations. Only the difficulties caused by multiplicity are maintained in the complex molecules, which are frequently deprived of symmetry and undergo great deformations after optical transition. The data considered above (Section 9)[45, 58, 60–62] on relaxational spectra show that the uncertainty $\delta V$ in the transition region $\lambda$ approaches the values $\delta V \approx 5000\,\mathrm{cm}^{-1}$, that is the relaxation probabilities $W_r^{e*} \approx 10^{15}\,\mathrm{s}^{-1}$.

The magnitude of Stokes shift, evaluated approximately from the distance between the absorption and fluorescence band maxima, shows that the above-mentioned rather fast relaxations occur at relatively small values $Q^* \approx 3000\,\mathrm{cm}^{-1}$ in the spectra under consideration. As was pointed out by Hochstrasser and Marzacco[58], the theories based on the Born–Oppenheimer approximation, even as initial ones, are in contradiction to this fact, which is, however, in good agreement with the model treated here. This can be easily understood by taking into account the fact that strong vibronic interactions lead to high $\delta V$ values in the $\lambda$ region (*Figure 14*) and, therefore, bring the barrier $H$ down to very small values, if the zeroth vibronic levels of the interacting electronic states I and II are not far from each other. If the vibronic interactions I $\leftrightsquigarrow$ II are not so strong, the $\delta V$ values and therefore the vibronic relaxation probability $W^e$ grow with increase of the difference between the zeroth vibronic levels I and II in the families of related compounds. This defines 'the rule of energy gap'[74], which is frequently maintained for such systems.

It is obvious that the Σ-type states correspond to the 'large molecules' limit in Robinson's consideration[75] and to the 'statistical limit' in that of Jortner and Berry[76]. However, it should be noted that subdivision Δ, M, Σ, λ is based only on an important inner molecular property, which is the degree of independence of different vibrational and vibronic states. This subdivision, which is independent of any intra- and intermolecular processes, is significant for evaluating their probabilities and even the possibility of their existence.

**12.** The numerous electronic states of a polyatomic molecule are coupled by a network of interactions resulting in various electronic relaxations, i.e. radiationless transitions between these states. The most essential electronic relaxations taking place in the group of low electronic molecular states are shown in *Figure 19*, along with the optical transitions between these states.

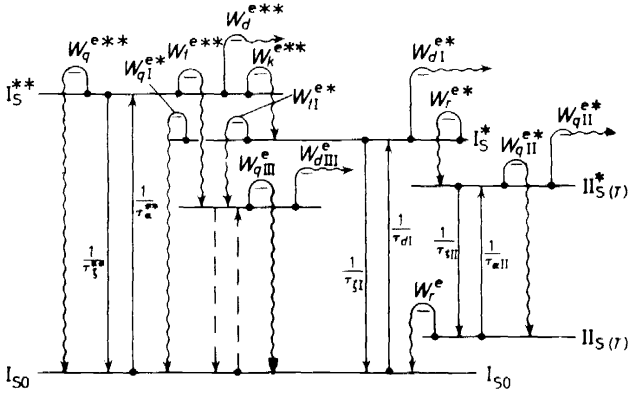


*Figure 19.* Essential electronic relaxations in the ground state and some of the low excited states of a polyatomic molecule. $(\tau_a)^{-1}$ and $(\tau_\zeta)^{-1}$ are the probabilities of the optical transitions, $W_i^e$ are the probabilities of the electronic relaxational transitions

The left-hand side and the centre of the scheme in *Figure 19* illustrate the ground and two excited singlet states $I_S$, $I_S^*$ and $I_S^{**}$ as well as a triplet one $III_T$. On the other side two more states $II_{S(T)}$ and $II_{S(T)}^*$ are shown, which together with the states $I_S$ and $I_S^*$ form the four-level scheme considered in part in the previous section (see *Figures 16* and *17*). The probabilities for the relaxations taking place here, that is the electronic rearrangements, are denoted in *Figure 19* as $W_r^{e*}$ and $W_r^e$. Notice that the systems of the states I, I* and II, II* can be differentiated by charge distribution (the $n\pi$ and $\pi\pi$ states) and can be of different symmetry and even of different multiplicity[45,54].

The other relaxations, namely, dissociation and ionization ($W_d^e$), transition from high excited electronic states to the first one ($W_k^e$), internal conversion to the ground state ($W_q^e$) and intersystem crossing ($W_i^e$), are widely accepted and their probabilities are well studied for a number of systems. Operating with the values of quantum yields of fluorescence $\eta_\zeta$, phosphorescence $\eta_\chi$ and primary photochemical process $\eta_\psi$, as well as with their temperature dependences and using the rate equations, it is possible to determine the probabilities $W_i^e$ for various electronic relaxations, based on the optical

transition probability values. The well-known results in this field are not discussed here. We shall only note some investigations, which have recently been possible in connection with the progress in experimental methods, involving fluorescence from the second excited level.

On the basis of critical consideration of numerous investigations of azulene luminescence, a scheme was suggested by Birks[77] describing the principal processes of excitation energy transformation in this molecule (*Figure 20*).

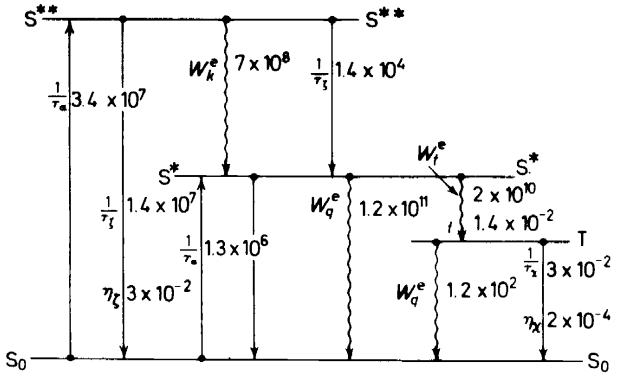


*Figure 20.* Main optical and relaxational transitions in azulene[77]

Relatively low optical transition and electronic relaxation probabilities enable the establishment of vibrational equilibrium in all the electronic states and, hence, the application of the rate equations for the analysis of the results (see also Section 10[63, 65]).

**13.** It seems to be advisable to present here a scheme of the origin of different types of vibronic spectra for several characteristic cases. The scheme in *Figure 21*[78] does not need detailed explanations. In the first three cases (*a–c*) the optical transitions occur between two equilibrium vibronic states and the spectra are described by two electronic levels. In the first case (*a*, the spectra $\Delta \rightarrow \Delta'$) the vibrational relaxations act, the probability of which is increased with increasing $Q$. In the second case (*b*, the spectra $\Delta \rightarrow M'$) the band diffusion is connected either with sequence congestion or with parametric relaxations. In the third case (*c*, the spectra $\Delta \rightarrow \Sigma'$) relatively large changes in the equilibrium configuration along the $r_m$-type coordinate result in the formation of continuous spectra which have latent vibrational structures. In cases *b* and *c* the deactivating of the vibrations of the $r_p$ and $r_m$ types by the vibrational relaxations is shown in the level systems.

The second group contains the molecules which in optical transition undergo rather strong changes in the cloud of valence electrons. These optical transitions connect the equilibrium initial states $\Delta$ with the quasi-stationary states ($\Delta'$ in case *d*, and $\Sigma'$ in case *e*), which once again equilibrate through the electronic rearrangements and vibrational relaxation chains. The spectra similar in shape to cases *a* and *c* are described by the four-level scheme, that is the frequencies $\nu_I^{00}$ and $\nu_{II}^{00}$ do not coincide and therefore the absorption and fluorescence spectra undergo an additional shift. These

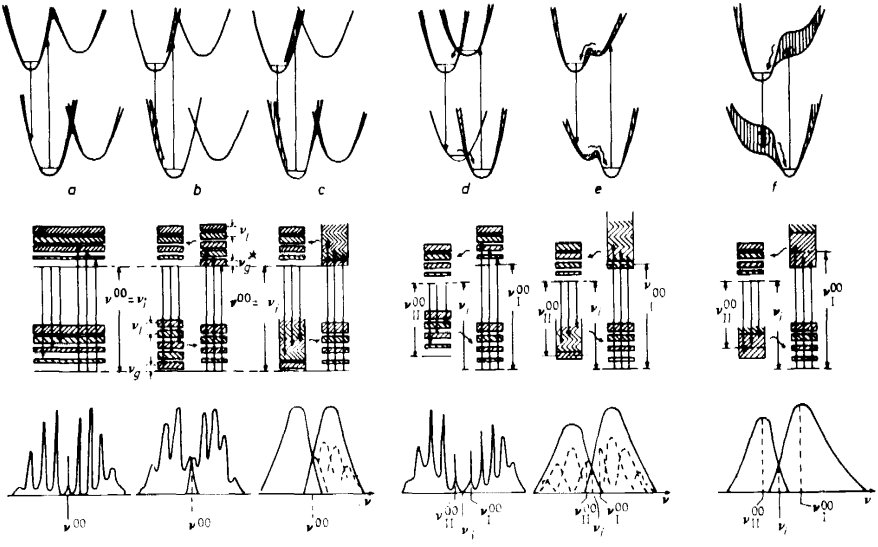


*Figure 21.* The formation of vibronic spectra for some typical cases[11, 78]

spectra are characterized by different values of the integral intensities $B_{el}$ and $B_{ell}$, and by various sets of vibrational frequencies.

In contrast to the configurational spectra *a–e*, case *f* describes the relaxational spectra, the origin of which has been discussed in detail in Section 9. A relatively narrow configurational distribution can only be displayed at the sides of these vibronic bands, just as narrow relaxational distributions are displayed at the sides of configurational spectra. The wavy arrows in schemes *d*, *e* and *f* indicate the vibronic relaxations and the vibrational ones that follow.

**14.** Apart from the qualitative considerations on the properties of vibronic spectra presented above, a quantitative description, based on the relationships between the absorption and fluorescence spectra, is possible.

The general relationship between the absorption and fluorescence spectra within the two-level scheme (*Figure 22*) was given by Stepanov[79]. The uncertain constants were excluded from this relationship by the present author and Mazurenko[80, 81]. The integral intensity relationship for these spectra was obtained in the most correct and useful form by Strickler and Berg[55].

The thermal equilibrium distribution among the vibrational states was assumed [55, 79–81]. Supposing that this distribution holds good for all the vibronic levels of both (I and II; I* and II*) pairs of partial states in the four-level scheme (*Figure 22*) and assuming an additive participation of these partial states in the summary spectra formation, the spectral and integral relationships can be expressed[7, 12] for the summary spectra in the case of the four-level scheme as follows:

$$\frac{\zeta_\nu}{\nu^3}\left[\frac{\eta_{\alpha\nu}\alpha_\nu}{\nu}\right]^{-1} = 2.89 \times 10^{-9}\mathcal{G}\mathcal{S}n_\nu^2\frac{\tau}{\eta_\zeta}\int \zeta_\nu \, d\nu \, 10^{-0.626(\nu-\nu_0)/T} \qquad (5)$$

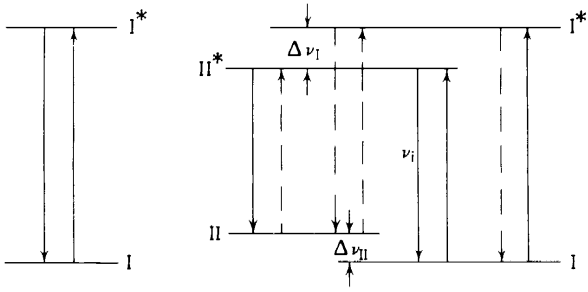


*Figure 22.* The two- and four-level schemes of electronic states; ———, crossing transitions between the level systems of the states I and II

$$\frac{\eta_\zeta}{\tau} = \frac{1}{\tau_\zeta} = \frac{1}{\mathscr{B}\tau_\alpha} = 2.89 \times 10^{-9} \frac{\mathscr{G}}{\mathscr{B}} \frac{n_\zeta^3}{n_\alpha} \frac{\int \zeta_\nu \, d\nu}{\int \frac{\zeta_\nu}{\nu^3} d\nu} \int \frac{\eta_{\alpha\nu}\alpha_\nu}{\nu} d\nu \tag{6}$$

$$\frac{\left[\int \frac{\zeta_\nu}{\nu^3} d\nu\right]^{-1} \frac{\zeta_\nu}{\nu^3}}{\left[\int \frac{\eta_{\alpha\nu}\alpha_\nu}{\nu} d\nu\right]^{-1} \frac{\eta_{\alpha\nu}\alpha_\nu}{\nu}} = \mathscr{S}\mathscr{B} \frac{n_\nu^2 n_\alpha}{n_\zeta^3} 10^{-0.626(\nu - \nu_i)/T} \tag{7}$$

$$\frac{\left[\tau_\zeta \int \frac{\zeta_\nu}{\nu^3} d\nu\right]^{-1} \frac{\zeta_\nu}{\nu^3}}{\left[\tau_\alpha \int \frac{\eta_{\alpha\nu}\alpha_\nu}{\nu} d\nu\right]^{-1} \frac{\eta_{\alpha\nu}\alpha_\nu}{\nu}} = \mathscr{S} \frac{n_\nu^2 n_\alpha}{n_\zeta^3} 10^{-0.626(\nu - \nu_i)/T} \tag{8}$$

Equation 5 may be applied to all the vibronic spectra, whereas equations 6–8 are applicable only to the symmetry-allowed spectra.

It is convenient to adopt the reversal lifetimes of the excited state as a general measure of the integral intensities of equilibrium vibronic absorption and emission spectra. For absorption spectra this lifetime $\tau_\alpha$ is calculated as the Strickler and Berg absorption integral (equation 6 with $\mathscr{B} = 1$). For fluorescence spectra $\tau_\zeta = \tau(\eta_\zeta)^{-1}$. Hence, according to equation 6[12,80] the necessary normalization of fluorescence and absorption spectra by their areas $F_\alpha$ and $F_\zeta$ under the relevant spectral curves is determined by the condition $F_\alpha\tau_\alpha = F_\zeta\tau_\zeta$.

The 'absorption yield' $\eta_\alpha$ is introduced into equations 5–8 for the exclusion of non-exciting absorption; $n$ is the index of refraction of the system under consideration, $(n_\alpha)^{-1}$ and $(n_\zeta^3)^{-1}$ are the values of $n^{-1}$ and $(n^3)^{-1}$ averaged over the absorption and fluorescence spectra. The parameters $\mathscr{G}$, $\mathscr{S}$ and $\mathscr{B}$ are, respectively, the relationships of the electronic statistical weights (multiplicities) $g_e/g_e^*$, the partition function $\zeta/\zeta^*$ and the optical transition probabilities $(B_e/B_e^*) = (\tau_\zeta/\tau_\alpha)$ for the summary ground and excited states, including both the partial states I and II. These parameter values for the two-level and four-level schemes are listed in *Table 1*. Therewith the possibility for optical cross-transitions between the levels of different partial states

*Table 1.*

| | Two-level system | Four-level system |
|---|---|---|
| $\mathscr{G}$ | $\frac{g_e}{g_e^*}$ | $\frac{g_{el}}{g_{ell}^*}$ |
| $\mathscr{S}$ | $\frac{s}{s^*}$ | $\frac{1}{\mathscr{G}}\frac{g_{el}s_I + g_{ell}s_{II}\,e^{-(h/kT)\Delta\nu_{II}}}{g_{el}^*s_I^* e^{-(h/kT)\Delta\nu_I} + g_{ell}^*s_{II}^*}$ |
| $\mathscr{B}$ | 1 | $\frac{1}{\mathscr{G}\mathscr{S}}\frac{g_{el}s_I(B_{el} + B_{el-II}) + g_{ell}s_{II}(B_{ell} + B_{ell-I})\,e^{-(h/kT)\Delta\nu_{II}}}{g_{el}^*s_I^*(B_{el}^* + B_{el-II}^*)\,e^{-(h/kT)\Delta\nu_I} + g_{ell}^*s_{II}^*(B_{ell}^* + B_{ell-I}^*)}$ |

I and II is also assumed. As was pointed out earlier, the states I and II (*Figure 22*) can be of various multiplicity, that is the values of $\mathscr{G} = \frac{1}{3}$, 1 and 3 are possible. The values of $\mathscr{S}$ are worthy of distinctive analysis. It need only be noted here that strong deviations from the value of $\mathscr{S} = 1$ are possible if one of the normal vibrations changes into libration, as a result of a relaxational transition I $\leftrightsquigarrow$ II. Supposing $\mathscr{B} = 1$, then equations 5–8 become the known ones for the two-level scheme[55, 79–81]. Therefore, the breaking of equation 6 at $\mathscr{B} = 1$, that is the difference in the values of $\tau_\alpha$ and $\tau_\zeta$ gives rise to a possible necessity for the application of the four-level scheme.

Lastly, it should be particularly emphasized that equations 5–8 are not directly applicable to the spectra formed in transitions to the mixed states, which have been formed in strong interactions, since these states cannot be considered as a simple sum of the partial ones. This problem will be reported in a following communication.

**15.** There are now many, varied results of application of the Strickler–Berg integral relationship[55] to two-level molecular systems. The spectral relationships[79–81], providing a means for determination of the position of the frequency $\nu_i$ in the continuous spectra, have not been so frequently applied. We shall consider the application of equations 6–8 to more complicated molecules, which are described by the three-level or four-level schemes. New data have been recently obtained relating to the systems which have already been described[78, 82]. Therefore it is advantageous to treat these examples once again.

*Figure 23* shows the spectra of triphenylbenzene in heptane reconstructed[82] from the data of Berlman[83], according to which $\tau_\zeta = 158$ ns. The $\tau_\alpha$ value calculated from the whole absorption band is $\tau_\alpha = 1.1$ ns. However, this band is easily divided into two components, the first of which $\alpha'_\nu$ (marked in *Figure 23* by the chain-dotted line) is characterized by $\tau_\alpha = 160\,\text{ns} \approx \tau_\zeta$ and gives the value of $\nu_I^{00} = 30800\,\text{cm}^{-1}$, determined by the point of intersection of $\alpha_\nu$ and $\zeta_\nu$ of the normalized spectra. The second absorption band, originated from the same ground state, is characterized by $\nu_{II}^{00} > \nu_I^{00}$. Thus, this system is a trivial scheme I–I*–I** with the second absorption band overlapping the first one.

The possibility of a four electronic level determination is illustrated by the spectra of some diphenylpolyene solutions given in *Figure 24*. These spectra are reconstructed[82] from the data of Berlman[83], Nikitina, Ter-Sarkisyan

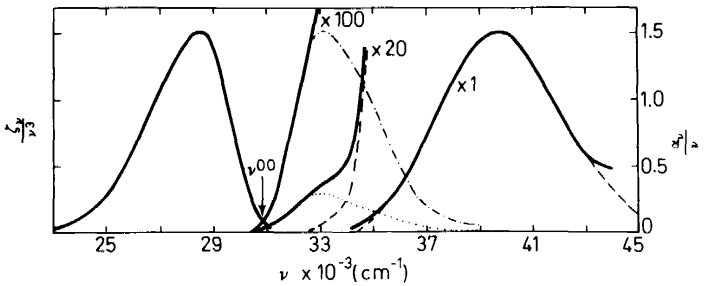


*Figure 23.* The spectra of triphenylbenzene in heptane reconstructed[82] from the data of Berlman[83]

*et al.*[84], and Birks and Dayson[85]. The broken lines represent the fluorescence spectra normalized by the height of their maxima and the solid lines represent those normalized by their areas, in accordance with equation 6, with the $\tau_\zeta$ values being taken from the data[83–85] and the $\tau_\alpha$ values calculated from the absorption spectra of *Figure 24* taking $\mathscr{B} = 1$ in equation 6. As a result, the $\nu_i$ values are derived from the normalized-spectra crossing. If the first sub-

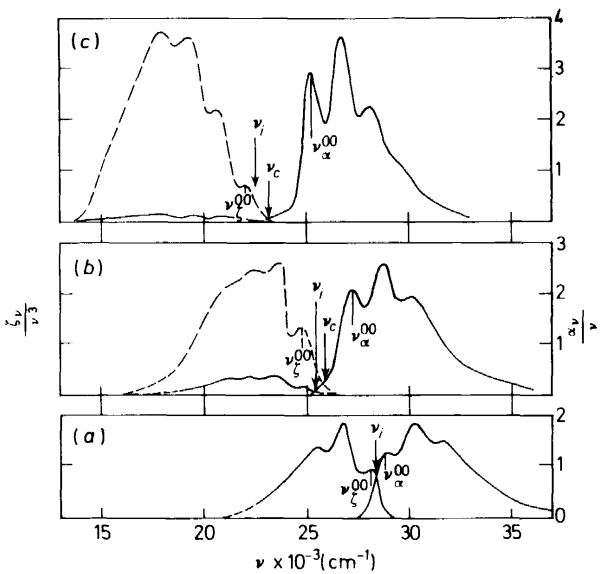


*Figure 24.* The spectra of diphenylpolyenes in heptane, reconstructed[82] from recent data[83–85]; (*a*) -diphenylbutadiene, (*b*) —diphenylhexatriene, (*c*) —diphenyloctatetraene

band maxima in the absorption and fluorescence spectra coincide with the $\nu_{\mathrm{I}}^{00}$ and $\nu_{\mathrm{II}}^{00}$ values, then it is easy to obtain a level structure of the considered compounds (shown in *Figure 25*). Here the cross-transitions between the levels of the partial states I and II are probably the Franck–Condon forbidden ones. Some basic data and the molecular characteristics obtained are listed

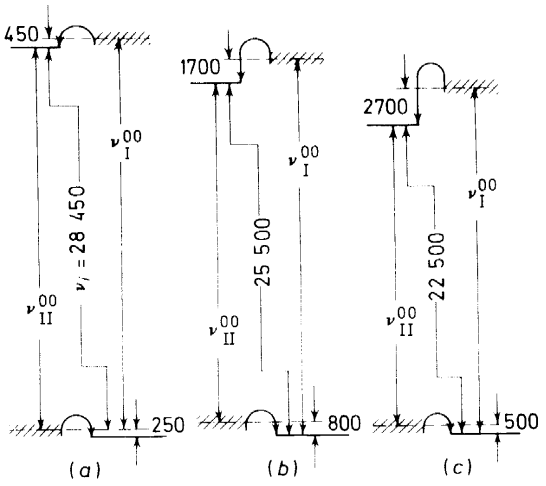


*Figure 25.* Levels for the molecules (*a*), (*b*), (*c*) of *Figure 24*[82]

in *Table 2*. It is evident that the spectra considered are described very well by the four-level scheme, which eliminates all the contradictions caused by discrepancies between the $\tau_\zeta$ and $\tau_\alpha$.

Recently Hudson and Kohler[86] found an additional weak-structured band in the absorption spectrum of diphenyloctatetraene in the dibenzyl host crystal. The onset of the band coincides with the origin of the fluorescence

*Table 2.* Diphenylpolyenes in hydrocarbon solvents

| Substance | $\nu_i$ ($cm^{-1}$) | $\nu_I^{00}$ ($cm^{-1}$) | $\nu_{II}^{00}$ ($cm^{-1}$) | $\tau_\alpha$ (ns) | $\tau_\zeta$ (ns) | $\mathscr{B}$ |
|---|---|---|---|---|---|---|
| Diphenylbutadiene (*a*) | 28450 | 28900 | 28200 | 1.5 | 1.8 | 1.2 |
| Diphenylhexatriene (*b*) | 25500 | 27200 | 24700 | 2.3 | 16.3 | 7.1 |
| Diphenyloctatetraene (*c*) | 22500 | 25200 | 22000 | 3.7 | 89 | 18.7 |

spectrum and is displaced by approximately 1100 $cm^{-1}$ to the blue from the main absorption band, which is also 50 times more intense (at 77 K). In the heptane solution at room temperature this relationship is $\tau_\zeta/\tau_\alpha = 18.7$ (*Table 2*). These facts are in full concordance with the four-level scheme.

Temperature investigations are desirable here as well. It should be noticed that according to the data of Schmid and Brosa[87] the 1600 $cm^{-1}$ Raman line, which is ascribed[88] to full-symmetrical vibrations in the polyene chain, undergoes a sharp increase in intensity in the pre-resonance region of excitation (16000–21000 $cm^{-1}$), the increase being sharp for diphenyloctatetraene in $CCl_4$ near 21000 $cm^{-1}$. It denotes firstly that an actual transition is situated in the region close to $\nu_{II}^{00}$, if the difference in solvents is taken into account, and secondly that variations in the polyene chain configuration take place in the transitions between the I and II states. All these facts prove the interpretation suggested in ref. 82.

**16.** An interesting complicated case is represented by the spectra of *trans*-retinol in isopentane (*Figure 26*) reconstructed[78] from the data of Thomson[89] and Dalle and Rosenberg[90]. In addition to differences in $\tau_\zeta$ and $\tau_\alpha$, this system is characterized[90] by a sharp temperature dependence of the

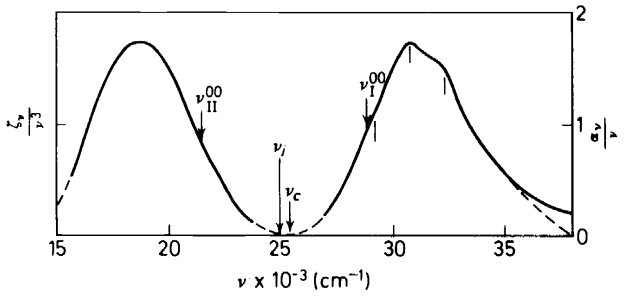


*Figure 26.* The absorption and fluorescence spectra of *trans*-retinol in isopentane, reconstructed[78] from recent data[89,90]: arrows denote the frequencies $\nu_I^{00}$ and $\nu_{II}^{00}$ calculated by the method of Klochkov and Korotkov[91]

value of $\tau_\alpha$. A rise in the temperature $T$ from approximately 70 K to 300 K is accompanied by a linear increase in $\tau_\zeta$ from 40 ns to 200 ns. Therewith, the value of $\tau_\zeta = 2.7$ ns is practically independent of temperature.

The temperature variations of $\tau_\zeta$ are ascribed[90] to lower probabilities for vibronic transitions from high vibrational levels of an excited state. It is hard to prove such an assumption.

It has been shown[78] that all the experimental data for *trans*-retinol can be completely explained in terms of the four-level diagram of *Figure 27*. According to this diagram the measured fluorescence quantum yield $\eta_\zeta$ is determined by radiationless transitions in two excited electronic states being

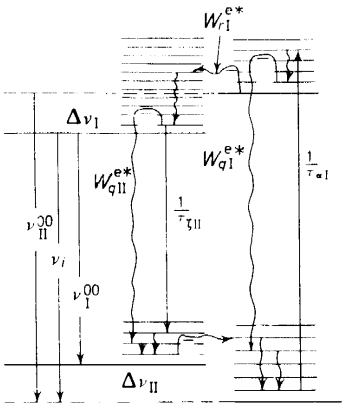


*Figure 27.* The scheme of levels and of optical and relaxational transitions in a *trans*-retinol molecule[78]

successively realized, that is in the Franck–Condon state I* and in the stationary state II*, i.e.

$$\eta_\zeta = \frac{W_{r\mathrm{I}}^{e*}}{W_{r\mathrm{I}}^{e*} + W_{q\mathrm{I}}^{e*}} \cdot \frac{A_{\mathrm{II}}}{A_{\mathrm{II}} + W_{q\mathrm{II}}^{e*}} \tag{9}$$

Here, the probabilities $W_{q\mathrm{I}}^{e*}$ and $W_{q\mathrm{II}}^{e*}$ represent the relaxations causing deactivation of the states I* and II*. An electronic rearrangement populates the level II* with the probability $W_{r\mathrm{I}}^{e*}$. Determined by Klochkov and Korotkov's method[91], the values of $\nu_{\mathrm{I}}^{00}$ and $\nu_{\mathrm{II}}^{00}$ (*Figure 27*) show that both the direct and inverse optical transitions occur completely in different systems of the levels (I and II), as $\Delta\nu_{\mathrm{I}}, \Delta\nu_{\mathrm{II}} \gg kT$. In all calculations it was assumed that the *trans*-retinol molecule is complex and that the probabilities for all electronic relaxations have an exponential temperature dependence, which is governed by their barrier heights (*Figure 27*). The calculations show that the complex exponential temperature relationships between the characteristics of the *trans*-retinol molecule, obtained in equation 9, are followed. The values of $A_{\mathrm{I}} = (\tau_\alpha)^{-1}$ and $A_{\mathrm{II}} = (\tau_{\zeta\mathrm{II}})^{-1}$, as well as those of the electronic relaxation probabilities shown in *Figure 27* and of the corresponding barrier heights are summarized in *Table 3*, along with the values of $\nu_i$, $\nu_{\mathrm{I}}^{00}$ and $\nu_{\mathrm{II}}^{00}$.

*Table 3. Trans*-retinol in isopentane solvent

| $\nu_i$ | $\nu_{\mathrm{I}}^{00}$ | $\nu_{\mathrm{II}}^{00}$ | $A_{\mathrm{I}}$ | $\left(\frac{W_{q\mathrm{I}}^{e*}}{W_{r\mathrm{I}}^{e*}}\right)_\infty$ | $H_{q\mathrm{I}}^{*} - H_{r\mathrm{I}}^{*}$ | $A_{\mathrm{II}}$ | $(W_{q\mathrm{II}}^{e*})_\infty$ | $H_{q\mathrm{II}}^{*}$ | $\mathscr{B}$ |
|---|---|---|---|---|---|---|---|---|---|
| ($cm^{-1}$) | ($cm^{-1}$) | ($cm^{-1}$) | ($s^{-1}$) | | ($cm^{-1}$) | ($s^{-1}$) | ($s^{-1}$) | $cm^{-1}$ | |
| 25000 | 28800 | 21500 | $3.7 \times 10^8$ | 20 | 150 | $4.9 \times 10^7$ | $7.5 \times 10^9$ | 480 | 7.5 |

Thus the suggested interpretation accounts for all the complex experimental data with no contradictions. Moreover, a number of constants concerning the light energy transformations in *trans*-retinol molecules, have been obtained. It is of interest that Rimai, Heyde, Heller and Gill[92] have found the excitation efficiency maximum near 20300 $cm^{-1}$ for the Raman line $\nu = 1587$ $cm^{-1}$ in the ethanolic solution of *trans*-retinol. The intense absorption bands are displaced in ethanolic solution to the red side compared to those in isopentane. Hence, one can suppose, just as in diphenylbutadiene, that the transition in the system II ($\nu_{\mathrm{II}}^{00} = 21500\,cm^{-1}$) is actually here. This seems no less probable than an assumption of these authors[92] on the influence of the excited triplet level, which must have been situated near 20000 $cm^{-1}$. Similar to the later results[87] obtained for diphenylpolyenes (see above, Section 15), the pre-resonance dependences of the line $\nu = 1578\,cm^{-1}$ point toward the changes of the polyene chain conformations in the transitions of the *trans*-retinol molecule between the states I and II.

**17.** In conclusion, the approximate estimates of probabilities for the vibrational and electronic relaxations are summarized in *Table 4* for some molecules of different complexity.

All of these estimations are approximated not only by numerical values, but also by a physical sense of the probabilities determined. So, some

*Table 4.*

| Substance | State | Character of vibronic spectra | Relaxation probabilities ($s^{-1}$) | | | |
|---|---|---|---|---|---|---|
| | | | $W^{v}_{\Delta}$ | $W^{v*}_{\Delta}$ | $W^{v*}_{\Sigma}$ | $W^{e**}_{\ddagger}$ |
| Benzene | Vap. | Discrete | — | $10^{6}$ (*b*, *c*) | — | $10^{7}$ (*h*) |
| Aniline | Vap. | Discrete | — | $10^{8}$ (*c*) | — | $10^{8}$ (*h*) |
| β-Naphthylamine | Vap. | Diffuse | — | $10^{8}$ (*d*) | $\gtrsim 10^{10}$ (*d*)† | $10^{8}$ (*h*) |
| Cryptocyanine | Sol. | Strongly diffuse | $\lesssim 10^{11}$ (*a*)* | $10^{11}$ (*e*) | $10^{11}$–$10^{13}$ (*a*) | — |
| Rhodamine 6G | Sol. | Strongly diffuse | — | $10^{11}$ (*e*, *f*) | $10^{12}$–$10^{13}$ (*f*) | — |
| 3-Aminophthalimide | Vap., sol. | Continuous | — | $10^{11}$ (*d*, *e*) | $10^{11}$–$10^{13}$ (*d*)† | $10^{10}$ (*i*) |
| Phthalocyanine–AlCl | Sol. | Strongly diffuse | — | — | $>10^{12}$ (*g*) | $10^{14}$ (*j*) |
| 3,6-Tetramethyldiaminophthalimide | Vap., sol. | Continuous (relaxational) | — | — | $>10^{12}$ (*g*) | $10^{15}$ (*k*) |

(*a*) from photobleaching and 'hole burning'[41, 42]
(*b*) from discharge emission spectra[27]
(*c*) from the resonance fluorescence existence[16–27]
(*d*) from the equivalency $(\nu_z, T)$[5, 33]
(*e*) from stimulated emission spectra kinetics[36–40]
(*f*) from the inverse population and amplification growth[34, 35]
(*g*) from the absence of stimulated emission spectra kinetics[36, 40]
(*h*) from the yield $\eta_z$ and the fluorescence duration $\tau$[5, 15, 18]
(*i*) $W^{e**}_{t} + W^{e**}_{q}$(?) from the yield $\eta_z$ and the absorption integral $\tau_z$[50]
(*j*) $W^{e**}_{t} + W^{e**}_{q}$(?) from homogeneous broadening of the vibronic maximum[41]
(*k*) $W^{e**}_{r}$ from homogeneous broadening of the vibronic band[7, 45]

* There are some contradictions in the literature (cf. the present paper and Ref. 43)
† Increased as a consequence of the formation of the mixed vibronic states
‡ The data for the $\nu_z$ frequencies, which slightly exceed $\nu^{00}$

electronic relaxations taking place from the thermalized states should be characterized by the values of $W^{e}_{\infty}$ and $H^{e}$, which describe the process with a better approximation than the value of $W^{e}$ given in *Table 4* for an initial state being not quite exact. As we have already pointed out, the vibrational relaxation probabilities depend to a larger degree on the vibrational state K in the cases $\Delta$ and M or on the instantaneous configuration $R$ in the case $\Sigma$, than on the mean vibrational energy store. The generalized probability $W^{v}$ choice, instead of a set of different probabilities $W^{v}(K)$, is brought about by the attention which is being given to the region of faster electronic relaxations and of the $\Sigma$-type states (continuous vibronic spectra).

In spite of these simplifications the tabulated data facilitate orientation in various and rather complex relaxational processes following optical transitions in a polyatomic molecule, and are sometimes competitive with them. The dynamics of these processes is determined by the existence and the properties of many non-stationary mixed vibronic and vibrational molecular states, which do not obey Born–Oppenheimer separation, since the more studied stationary pure Born–Oppenheimer states mainly define the molecular statics.

In the considered sense the principal features of complex polyatomic molecules do not depend upon the existence of many partial electronic states. Such sets of states are inherent in some simple polyatomic and even diatomic molecules. The main peculiarities of the polyatomic molecule, as a labile relaxing system, are determined by its many normal vibrations which possess different properties and which perform various functions in energy transformation processes. These functions are, for example, the role of a passive 'heat bath' as well as of a distributional network associating by different ways the normal vibrations with each other and with a system of valence electrons, and the formation of the canals, that is 'bottle necks', through which the definite changes in molecular structure take place. These and many other functions are intimately connected with the existence of mixed states, the latter being sometimes rather broad, but in other cases they are strongly restricted along the molecular configurations and energies.

The quantity of possible states and the probabilities for their relaxational interactions are increased with molecular complexity, that is with an increasing number of forming atoms, with decreasing symmetry and rigidity of the carbon skeleton and, to a great extent, with increasing number, activity and position asymmetry of substituent groups. It is because of this that more simple molecules display their inner features only under conditions of diluted vapour. More complicated molecules maintain these features even in solution. In this case the external effects are weaker than the inner interactions.

The consideration of the experimental evidence is not complete and is restricted not only in the number of examples but also in the citation of various methods. Meanwhile, the complexity of molecules and the processes taking place in them need further investigations, so that a more detailed picture of the phenomena can be obtained.

The molecular complexity and high energies of intramolecular relaxational interactions, which sometimes greatly exceed the difference in energy of the interacting states, are not excepted to cause difficulties in the application of the existing theories to the mixed molecular states. As we have already

mentioned, here the semiclassical statistical theories may be productive and in better agreement with the model of the object under examination.

## REFERENCES


[1] B. Henri and M. Kasha, *Ann. Rev. Phys. Chem.* **19**, 161 (1968).
[2] J. Jortner, S. A. Rice and R. M. Hochstrasser, *Adv. Photochem.* 7, 149 (1969).
[3] E. Fermi, *Z. Physik.* **71**, 150 (1931).
[4] G. P. Ittman, *Naturwiss.* **22**, 118 (1934).
[5] B. S. Neporent, *Thesis* (1945); *Zh. Fiz. Khim.* **21**, 1111 (1947).
[6] F. Fischer and E. W. Schlag, *Chem. Phys. Letters*, **4**, 393 (1969).
[7] B. S. Neporent, *Molecular Photonics*, p. 18, Nauka, Leningrad (1970).
[8] B. S. Neporent, *Opt. Spectr.* **32**, 19 (1972).
[9] B. S. Neporent, *Opt. Spectr.* **32**, 133 (1972).
[10] B. S. Neporent, *Opt. Spectr.* **32**, 240 (1972).
[11] B. S. Neporent, *Opt. Spectr.* **32**, 355 (1972).
[12] B. S. Neporent, *Opt. Spectr.* **32**, 468 (1972).
[13] E. Fermi, *Notes on Quantum Mechanics*, Univ. of Chicago Press (1960).
[14] J. C. Vinans and E. C. G. Stueckelberg, *Proc. Nat. Acad. Sci. US*, **14**, 867 (1928).
[15] A. N. Terenin, *Zh. Fiz. Khim.* **18**, 1 (1944).
[16] G. B. Kistiakowski and M. Nelles, *Phys. Rev.* **41**, 595 (1932).
[17] P. Pringsheim, *Ann. Acad. Warsaw*, **5**, 29 (1938).
[18] A. T. Vartanyan, *Izv. Akad. Nauk SSSR, Ser. Fiz.* 341 (1938).
[19] C. S. Parmenter and M. W. Shyuler, *J. Chem. Phys.*, **52**, 5366 (1970).
[20] B. K. Selinger and W. R. Were, *J. Chem. Phys.* **52**, 5482 (1970).
[21] K. G. Spears and S. A. Rice, *J. Chem. Phys.* **55**, 5561 (1971).
[22] M. Quack and M. Stockburger, *J. Mol. Spectr.* **43**, 87 (1972).
[23] E. W. Shlag, S. Schneider and D. W. Chandler, *Chem. Phys. Letters*, **11**, 474 (1971).
[24] S. O. Mirumyantz, Abstracts of the XIth European Congress on Molecular Spectroscopy, 26 (B1), Akad. Nauk Est. SSR, Tallinn (1973).
[25] H. Weyssenhoff and F. Krauss, *J. Chem. Phys.* **54**, 2387 (1972).
[26] V. P. Klochkov, *Opt. Spectr.* **24**, 19 (1968).
[27] M. Stockburger, *Ber. Bunsenges.* **72**, 151 (1968).
[28] G. M. Breuer and E. K. C. Lee, *Chem. Phys. Letters*, **14**, 404 (1972).
[29] D. S. McClure, *J. Chem. Phys.* **17**, 905 (1949).
[30] E. W. Shlag and H. Weyssenhoff, *J. Chem. Phys.* **51**, 2508 (1968).
[31] M. Boudart and J. T. Dubois, *J. Chem. Phys.* **23**, 223 (1955).
[32] B. Stevens, *J. Chem. Phys.* **24**, 488 (1956).
[33] B. S. Neporent, *Thesis* (1945); *Zh. Fiz. Khim.* **24**, 1219 (1950).
[34] M. R. Topp, P. M. Rentzepis and R. P. Jones, *Chem. Phys. Letters*, **9**, 1 (1971).
[35] D. Ricard, W. H. Lowdermilk and J. Ducuing, *Chem. Phys. Letters*, **16**, 617 (1972).
[36] B. S. Neporent and V. B. Shilov, *Opt. Spectr.* **30**, 576 (1971).
[37] B. S. Neporent, V. V. Kryukov, G. V. Lukomskii and V. B. Shilov, Abstracts of the VIth Conference on Non-linear Optics, p. 107, Minsk (1972).
[38] B. S. Neporent, V. B. Shilov and G. V. Lukomskii, Abstracts of XVII Conference on Spectroscopy, p. 27, Minsk, USSR (1971).
[39] M. Bass and J. I. Steinfeld, *J. Quant. Electron.* **QE-4**, 53 (1968).
[40] W. E. Gibbs and H. E. Kellock, *J. Quant. Electron.* **QE-4**, 293 (1968).
[41] M. Spaeth and W. Sooy, *J. Chem. Phys.* **48**, 2315 (1968).
[42] C. Giuliano and J. Hess, *Appl. Phys. Letters*, **9**, 196 (1966).
[43] T. K. Razumova and N. O. Skorobogatov, Abstracts of Symposium on Stimulated Emission Frequency Controlling, 92, Institute of Physics of Acad. of Sci. Ukr. SSR, Kiev (1972).
[44] J. Christoffersen, J. M. Hollas and G. H. Kirby, *Mol. Phys.* **16**, 441 (1969).
[45] B. S. Neporent, *Zh. Eksperim. i Teor. Fiz.* **22**, 172 (1951).
[46] J. P. Byrne and I. G. Ross, *Austral. J. Chem.* **24**, 1107 (1971).
[47] N. A. Borisevich and V. A. Tolkachev, *Dokl. Akad. Nauk BSSR*, **7**, 87 (1963).
[48] V. A. Tolkachev and N. A. Borisevich, *Opt. Spektroskopiya*, Suppl. **1**, 22 (1963); **18**, 388 (1965).
[49] V. A. Tolkachev, *Izv. Akad. Nauk SSSR, Ser. Fiz.* **27**, 584 (1963).
[50] B. S. Neporent and N. A. Borisevich, *Opt. Spektroskopiya*, **1**, 143 (1956).

[51] B. S. Neporent, V. V. Zelinskii and V. P. Klochkov, *Dokl. Akad. Nauk SSSR*, **92**, 927 (1953).
[52] B. S. Neporent, V. P. Klochkov and O. A. Motovilov, *Zh. Fiz. Khim.* **24**, 305 (1955).
[53] B. S. Neporent, N. G. Bakhshiev, V. A. Lavrov and S. M. Korotkov, *Opt. Spektroskopiya*, **13**, 31 (1962).
[54] B. S. Neporent, *Izv. Akad. Nauk SSSR, Ser. Fiz.* **15**, 533 (1961).
[55] S. J. Strickler and R. A. Berg, *J. Chem. Phys.* **37**, 814 (1962).
[56] N. Z. Marek, *Z. Naturforsch.* **19a**, 371 (1964).
[57] A. N. Sevchenko, G. P. Gurinovich and A. M. Sarzhevskii, *Dokl. Akad. Nauk SSSR*, **127**, 1191 (1964).
[58] R. Hochstrasser and C. Marzacco, *J. Chem. Phys.* **49**, 971 (1968).
[59] M. Kasha, *Discussions Faraday Soc.* **9**, 14 (1950).
[60] B. S. Neporent, *Zh. Fiz. Khim.* **30**, 1048 (1956).
[61] P. P. Feofilov and I. G. Faerman, *Dokl. Akad. Nauk SSSR*, **87**, 931 (1952).
[62] E. N. Victorova and I. A. Gofman, *Zh. Fiz. Khim.* **34**, 2643 (1965).
[63] H. Baba, A. Nakajima, M. Aoi and K. Chihara, *J. Chem. Phys.* **55**, 2433 (1971).
[64] M. D. Galanin and Z. A. Chizhikova, Short Communications of Institute of Physics of the Acad. Sci. USSR, No. 4, 35 (1971).
[65] M. D. Galanin and Z. A. Chizhikova, *Izv. Akad. Nauk SSSR, Ser. Fiz.* **36**, 941 (1972).
[66] R. Heiligman, *Abhandl. Deutsch. Akad. Wiss, Berlin Kl. Math. Physik. Tech.* **7**, 265 (1967).
[67] C. Balny, K. Dzhaparidze and P. Douzou, *CR Acad. Sci., Paris*, **265**, 1148 (1967).
[68] E. C. Lim, Y. H. Li and R. Li, *J. Chem. Phys.* **53**, 2443 (1970).
[69] K. K. Innes, J. D. Simmons and S. G. Tilford, *J. Mol. Spectros.* **11**, 257 (1963).
[70] K. K. Innes and J. E. Parkin, *J. Mol. Spectr.* **21**, 66 (1966).
[71] M. Ito, I. Suzuka, Y. Udagava, N. Mikami and K. Kaya, *Chem. Phys. Letters*, **16**, 211 (1972).
[72] A. N. Kalantar, E. S. Franzosa and K. K. Innes, *Chem. Phys. Letters*, **17**, 335 (1972).
[73] A. C. Albrecht, *J. Chem. Phys.* **34**, 1476 (1961).
[74] W. Siebrand, *J. Chem. Phys.* **47**, 2411 (1967).
[75] G. W. Robinson, *J. Chem. Phys.* **47**, 1967 (1967).
[76] J. Jortner and R. S. Berry, *J. Chem. Phys.* **48**, 2537 (1968).
[77] J. B. Birks, *Chem. Phys. Letters*, **17**, 370 (1972).
[78] B. S. Neporent, *Izv. Akad. Nauk SSSR, Ser. Fiz.* **38**, 276 (1973).
[79] B. I. Stepanov, *Dokl. Akad. Nauk SSSR*, **112**, 839 (1957); *Izv. Akad. Nauk SSSR, Ser. Fiz.* **22**, 1367 (1958).
[80] B. S. Neporent, *Izv. Akad. Nauk SSSR, Ser. Fiz.* **22**, 1372 (1958).
[81] Yu. T. Mazurenko and B. S. Neporent, *Opt. Spektroskopiya*, **12**, 571 (1962).
[82] B. S. Neporent, *Izv. Akad. Nauk SSSR, Ser. Fiz.* **36**, 929 (1972).
[83] I. Berlman, *Handbook of Fluorescence Spectra of Aromatic Molecules*, Academic Press, New York (1965).
[84] A. N. Nikitina, G. S. Ter-Sarkisyan, B. M. Mikhailov and L. E. Minchenkova, *Opt. Spektroskopiya*, **24** 655 (1968).
[85] J. B. Birks and B. J. Dayson, *Proc. Roy. Soc.* **275A**, 136 (1963).
[86] B. S. Hudson and B. E. Kohler, *Chem. Phys. Letters*, **14**, 299 (1972).
[87] E. D. Schmid and B. Brosa, *J. Chem. Phys.* **58**, 637 (1973).
[88] P. P. Shorygin and T. M. Ivanova, *Opt. Spectr.* **25**, 107 (1968).
[89] A. J. Thomson, *J. Chem. Phys.* **51**, 4106 (1969).
[90] J. P. Dalle and B. Rosenberg, *Photochem. Photobiol.* **12**, 151 (1970).
[91] V. P. Klochkov and V. A. Korotkov, *Opt. Spektroskopiya*, **20**, 582 (1966).
[92] L. Rimai, M. E. Heyde, H. G. Heller and D. Gill, *Chem. Phys. Letters*, **10**, 207 (1971).